journal of the international meteor organization

WGN

33:2
april 2005

Electrophonic meteors
Taurids
Ursids
IMC 2005

ISSN 1016-3115

WGN Vol. 33, No. 2, April 2005, pp. 33 – 66

Administrative

Conferences

Taurids

Electrophonic meteors

Ongoing meteor work

History

Front cover photo

A magnitude −3 Perseid photographed on 1986 August 13 from Pumichel, France. Camera: Canon T70; lens: Canon FD 50 mm $f/1.4$ S.S.C.; film Agfaprof 400. Reproduced by kind permission of the photographer, Koen Miskotte; see his website `http://home.planet.nl/~misko002/` .
Photographer's reference: 30403556.130819863Perseidmeteor.jpg.

Writing for WGN

This Journal welcomes papers submitted for publication. All papers are reviewed for scientific content, and edited for English and style. Instructions for authors can be found in WGN **31:4**, 124–128, and at `http://www.imo.net/articles/writingforwgn.pdf` .

Cover design

Rainer Arlt

Copyright

Editorial

Chris Trayner

The International Meteor Conference (IMC) is in Belgium this September. Outline details were announced in the previous WGN, but more information is now available.

There will be an invited lecture 'The Impact of Impacts' on asteroid and comet impacts and mass extinction events. This will be given by Prof. Dr. Philippe Claeys of the Vrije Universiteit, Brussel.

The Financial Support Fund for participants at IMC is operating again this year. This is offered to those who could not otherwise attend. The closing date for applications is June 20; note that it may not be possible to grant funds to all applicants.

Those who have been to IMC before know that it is a very pleasant opportunity to immerse oneself in meteor science for a long weekend and return refreshed and keen to carry on meteor work. The climate is very international: although the official language of the conference is English, it provides a chance to improve your Bulgarian, Chinese, French, German, Japanese, Romanian, Russian, Slovene, and probably other languages too. Newcomers are especially welcome.

Details of these matters, and of the rest of IMC 2005, can be found on page 35.

Letter: 2004 IMO Video Meteor Network data available

Sirko Molau[1]

After all 2004 data of the IMO Video Meteor Network have been collected, checked and archived, the data have been made available at `http://www.metrec.org/database.html` recently. The last year adds about 25 000 records from 351 observing nights to the database, which brings the total number of single station meteor records to almost 150 000 observed in more than 1 700 observing nights.

The data are available in IMO's PosDat format and can be fed directly into the Radiant software. If you are doing any type of meteor shower analysis or suspect some minor meteor shower activity, I strongly recommend you to download the corresponding data and check what you find in the video records. By now, each night of the year is covered by video data — in most cases from different years.

Solar Longitudes for 2005

Compiled by Rainer Arlt

A conversion table of dates to solar longitudes using (Steyaert, 1991) is given as every year. The longitudes are given on the next page; they are only valid for 2005. The conversion formulae for any time of the day are repeated here for your convenience.

If you want to calculate the solar longitude $\lambda_\odot$ of a specific time of the day, you may use a linear interpolation between two dates. Suppose you have a certain *Date* and the *Time* in hours (UT), you get the solar longitude by

$$\lambda_\odot = \lambda_{\odot,\mathrm{Date}} + (\lambda_{\odot,\mathrm{NextDay}} - \lambda_{\odot,\mathrm{Date}}) \times \frac{\mathrm{Time}}{24\ ^\mathrm{h}}.$$

Alternatively, if you want to convert a certain solar longitude $\lambda_\odot$ into a time of the day, look up the *Date* with the next-smaller solar longitude in the table and calculate

$$\mathrm{Time} = \frac{(\lambda_\odot - \lambda_{\odot,\mathrm{Date}})}{(\lambda_{\odot,\mathrm{NextDay}} - \lambda_{\odot,\mathrm{Date}})} \times 24\ ^\mathrm{h}.$$

The solar longitudes of 1988–2020 are given in 2-hour increments and with three decimals at `http://www.imo.net/solarlong`.

Reference

Steyaert, C. (1991), "Calculating the Solar Longitude 2000.0", *WGN* **19:2**, 31–34.

[1] *Abenstalstraße 13b, D-84072, Seysdorf, Germany. Email:* `Sirko@molau.de`

Solar longitudes 2005. Dates refer to 00^h UT.

Jan	1	280.60	Mar	1	340.43	May	1	40.65	Jul	1	99.20	Sep	1	158.59	Nov	1	218.59
Jan	2	281.62	Mar	2	341.43	May	2	41.62	Jul	2	100.15	Sep	2	159.56	Nov	2	219.59
Jan	3	282.64	Mar	3	342.44	May	3	42.59	Jul	3	101.10	Sep	3	160.53	Nov	3	220.59
Jan	4	283.66	Mar	4	343.44	May	4	43.56	Jul	4	102.06	Sep	4	161.50	Nov	4	221.59
Jan	5	284.68	Mar	5	344.44	May	5	44.53	Jul	5	103.01	Sep	5	162.46	Nov	5	222.60
Jan	6	285.70	Mar	6	345.44	May	6	45.50	Jul	6	103.97	Sep	6	163.43	Nov	6	223.60
Jan	7	286.72	Mar	7	346.44	May	7	46.47	Jul	7	104.92	Sep	7	164.41	Nov	7	224.60
Jan	8	287.73	Mar	8	347.44	May	8	47.44	Jul	8	105.87	Sep	8	165.38	Nov	8	225.61
Jan	9	288.75	Mar	9	348.45	May	9	48.41	Jul	9	106.83	Sep	9	166.35	Nov	9	226.61
Jan	10	289.77	Mar	10	349.44	May	10	49.37	Jul	10	107.78	Sep	10	167.32	Nov	10	227.62
Jan	11	290.79	Mar	11	350.44	May	11	50.34	Jul	11	108.73	Sep	11	168.29	Nov	11	228.62
Jan	12	291.81	Mar	12	351.44	May	12	51.31	Jul	12	109.69	Sep	12	169.26	Nov	12	229.63
Jan	13	292.83	Mar	13	352.44	May	13	52.27	Jul	13	110.64	Sep	13	170.24	Nov	13	230.63
Jan	14	293.85	Mar	14	353.44	May	14	53.24	Jul	14	111.60	Sep	14	171.21	Nov	14	231.64
Jan	15	294.87	Mar	15	354.44	May	15	54.20	Jul	15	112.55	Sep	15	172.18	Nov	15	232.65
Jan	16	295.89	Mar	16	355.43	May	16	55.17	Jul	16	113.50	Sep	16	173.16	Nov	16	233.65
Jan	17	296.91	Mar	17	356.43	May	17	56.13	Jul	17	114.46	Sep	17	174.13	Nov	17	234.66
Jan	18	297.92	Mar	18	357.42	May	18	57.09	Jul	18	115.41	Sep	18	175.11	Nov	18	235.67
Jan	19	298.94	Mar	19	358.42	May	19	58.06	Jul	19	116.37	Sep	19	176.09	Nov	19	236.68
Jan	20	299.96	Mar	20	359.41	May	20	59.02	Jul	20	117.32	Sep	20	177.06	Nov	20	237.68
Jan	21	300.98	Mar	21	0.41	May	21	59.98	Jul	21	118.27	Sep	21	178.04	Nov	21	238.69
Jan	22	301.99	Mar	22	1.40	May	22	60.94	Jul	22	119.23	Sep	22	179.02	Nov	22	239.70
Jan	23	303.01	Mar	23	2.39	May	23	61.90	Jul	23	120.18	Sep	23	179.99	Nov	23	240.71
Jan	24	304.03	Mar	24	3.38	May	24	62.86	Jul	24	121.14	Sep	24	180.97	Nov	24	241.72
Jan	25	305.04	Mar	25	4.37	May	25	63.82	Jul	25	122.09	Sep	25	181.95	Nov	25	242.74
Jan	26	306.06	Mar	26	5.36	May	26	64.78	Jul	26	123.05	Sep	26	182.93	Nov	26	243.75
Jan	27	307.08	Mar	27	6.35	May	27	65.74	Jul	27	124.00	Sep	27	183.91	Nov	27	244.76
Jan	28	308.09	Mar	28	7.34	May	28	66.70	Jul	28	124.96	Sep	28	184.89	Nov	28	245.77
Jan	29	309.11	Mar	29	8.33	May	29	67.66	Jul	29	125.91	Sep	29	185.88	Nov	29	246.79
Jan	30	310.12	Mar	30	9.32	May	30	68.62	Jul	30	126.87	Sep	30	186.86	Nov	30	247.80
Jan	31	311.14	Mar	31	10.31	May	31	69.58	Jul	31	127.83						
Feb	1	312.15	Apr	1	11.29	Jun	1	70.54	Aug	1	128.78	Oct	1	187.84	Dec	1	248.81
Feb	2	313.17	Apr	2	12.28	Jun	2	71.50	Aug	2	129.74	Oct	2	188.83	Dec	2	249.83
Feb	3	314.18	Apr	3	13.27	Jun	3	72.46	Aug	3	130.70	Oct	3	189.81	Dec	3	250.84
Feb	4	315.20	Apr	4	14.25	Jun	4	73.41	Aug	4	131.65	Oct	4	190.80	Dec	4	251.86
Feb	5	316.21	Apr	5	15.24	Jun	5	74.37	Aug	5	132.61	Oct	5	191.78	Dec	5	252.87
Feb	6	317.23	Apr	6	16.22	Jun	6	75.33	Aug	6	133.57	Oct	6	192.77	Dec	6	253.89
Feb	7	318.24	Apr	7	17.21	Jun	7	76.29	Aug	7	134.53	Oct	7	193.75	Dec	7	254.90
Feb	8	319.25	Apr	8	18.19	Jun	8	77.24	Aug	8	135.49	Oct	8	194.74	Dec	8	255.92
Feb	9	320.27	Apr	9	19.17	Jun	9	78.20	Aug	9	136.45	Oct	9	195.73	Dec	9	256.93
Feb	10	321.28	Apr	10	20.15	Jun	10	79.16	Aug	10	137.40	Oct	10	196.72	Dec	10	257.95
Feb	11	322.29	Apr	11	21.14	Jun	11	80.11	Aug	11	138.36	Oct	11	197.70	Dec	11	258.96
Feb	12	323.30	Apr	12	22.12	Jun	12	81.07	Aug	12	139.32	Oct	12	198.69	Dec	12	259.98
Feb	13	324.31	Apr	13	23.10	Jun	13	82.03	Aug	13	140.28	Oct	13	199.68	Dec	13	261.00
Feb	14	325.32	Apr	14	24.08	Jun	14	82.98	Aug	14	141.24	Oct	14	200.67	Dec	14	262.01
Feb	15	326.33	Apr	15	25.06	Jun	15	83.94	Aug	15	142.20	Oct	15	201.66	Dec	15	263.03
Feb	16	327.34	Apr	16	26.04	Jun	16	84.89	Aug	16	143.17	Oct	16	202.65	Dec	16	264.05
Feb	17	328.35	Apr	17	27.02	Jun	17	85.85	Aug	17	144.13	Oct	17	203.65	Dec	17	265.06
Feb	18	329.36	Apr	18	27.99	Jun	18	86.80	Aug	18	145.09	Oct	18	204.64	Dec	18	266.08
Feb	19	330.37	Apr	19	28.97	Jun	19	87.75	Aug	19	146.05	Oct	19	205.63	Dec	19	267.10
Feb	20	331.38	Apr	20	29.95	Jun	20	88.71	Aug	20	147.01	Oct	20	206.62	Dec	20	268.12
Feb	21	332.39	Apr	21	30.92	Jun	21	89.66	Aug	21	147.97	Oct	21	207.62	Dec	21	269.13
Feb	22	333.39	Apr	22	31.90	Jun	22	90.62	Aug	22	148.94	Oct	22	208.61	Dec	22	270.15
Feb	23	334.40	Apr	23	32.87	Jun	23	91.57	Aug	23	149.90	Oct	23	209.61	Dec	23	271.17
Feb	24	335.41	Apr	24	33.85	Jun	24	92.52	Aug	24	150.86	Oct	24	210.60	Dec	24	272.19
Feb	25	336.41	Apr	25	34.82	Jun	25	93.48	Aug	25	151.83	Oct	25	211.60	Dec	25	273.21
Feb	26	337.42	Apr	26	35.79	Jun	26	94.43	Aug	26	152.79	Oct	26	212.60	Dec	26	274.23
Feb	27	338.42	Apr	27	36.77	Jun	27	95.38	Aug	27	153.76	Oct	27	213.59	Dec	27	275.25
Feb	28	339.43	Apr	28	37.74	Jun	28	96.34	Aug	28	154.72	Oct	28	214.59	Dec	28	276.27
			Apr	29	38.71	Jun	29	97.29	Aug	29	155.69	Oct	29	215.59	Dec	29	277.28
			Apr	30	39.68	Jun	30	98.24	Aug	30	156.65	Oct	30	216.59	Dec	30	278.30
									Aug	31	157.62	Oct	31	217.59	Dec	31	279.32

Conferences

International Meteor Conference 2005 September 15–18, Oostmalle, Belgium

The IMC 2005 Committee

The first time

For the first time since the foundation of IMO, the International Meteor Conference will be held in Belgium, on September 15–18, 2005. Oostmalle is a Belgian village located 30 km northeast of the beautiful city of Antwerp, second largest city of Belgium, fourth largest port in the world, and the world capital of diamonds. Urania, the Public Observatory of Antwerp, has maintained regular contacts with IMO since 1988. Actually, Urania is IMO's official seat, and its meteor section is very proud to organize this IMC.

Go Belgian

The conference center 'Provinciaal Vormingscentrum' lies in a green area, and offers accommodation for 100 people or more (rooms for 1 to 6 persons). There is one big lecture hall and some smaller well-equipped rooms with Internet access. The evenings can be spent in the two cosy bars we have at our disposal. Beer lovers can taste a selection of the finest Belgian beers there.

The weather

The temperature is typically around 15–20 degrees Celsius (60-70 degrees Fahrenheit) in September.

Currency

The official currency in Belgium is the Euro. Foreign currency can be exchanged in banks and exchange offices.

Guest Lecture: 'The Impact of Impacts'

On Friday September 16 at 16^{h}, Prof. Dr. Philippe Claeys (Vrije Universiteit Brussel) will talk about 'The Impact of Impacts'. Professor Claeys is a geologist whose active research interests include the bio-geo-evolution of the Earth, global changes, rapid climatic changes and mass extinction events, effects of asteroid and comet impacts on the global Earth system, isotope geochemistry, stratigraphy/geochronology, sedimentology and sedimentary petrography, and planetary science. He is currently involved in some exciting research on the Chicxulub crater (Yucata'n, Mexico). See `http://we.vub.ac.be/~dglg/Web/Claeys/Claeys.htm`.

The excursion

A traditional part of the program is the excursion, which will lead us to the nice and small characteristic city of Lier, famous for its beguinage and the 'Zimmertoren'. Even Albert Einstein was impressed by this old tower in which Louis Zimmer built a whole range of high-quality astronomical clocks in the 1930s.

Participation fee

If you wish to register, please fill out the registration form on the next page or register online at the IMC 2005 website (see below). The participation fee for the IMC 2005 is €120 for people who register before July 1st and €130 for those who register later. This fee includes lodging, meals, excursion and the Proceedings. Either a prepayment of €60 or the total amount should be sent to IMO treasurer Ina Rendtel (details inside back cover and IMC 2005 website).

Visas and invitations

We will gladly send official invitations to people who need these to get a visa, provided that they inform us about this in due time. You can find out on the IMC website whether visa are required for citizens of your country.

Radio meteor school 2005

We proudly present the 'Radio Meteor School 2005', a five-day tutorial (Oostmalle, September 10 till 14) in which Prof. Dr. Oleg Belkovich, Russian eminence grise in meteor astronomy, will lecture on the physical and mathematical theory of radio meteor observations. We stress the fact that this is not an easy course, and it will

be helpful only to devoted radio observers highly skilled in mathematics and willing to get the utmost data out of their observations. For these people, it is very worthwhile to arrive in Belgium five days before the IMC to participate in the Radio Meteor School. The additional price will be around €150, and should only be paid upon arrival. However, you must register for this school before July 1st. Contact the organizers in order to register.

Contact information

For more information, check the IMC 2005 website at http://www.imo.net/imc2005 or contact the organizers by e-mail at imc2005@imo.net. You can also write to us: IMC 2005 — Jan Verbert, Public Observatory Urania, Jozef Mattheessensstraat 60, B-2540 Hove, Belgium.

Financial Support to Participants of the IMC 2005

As last year, *IMO* is making funds available to support attendance at the *IMC* 2005. To apply for support:

1. E-mail your application to *IMO* President Jürgen Rendtel, at `president@imo.net`. Include the word 'Meteor' in the subject line to get round the anti-spam filters. *IMO* cannot be held responsible for applications which are lost or arrive late. The application must be submitted by an *IMO* member, but may also request support for other meteor workers. The proposal must state that all the candidates are committed to attend the *IMC* (except for unforeseen circumstances) if the requested support is granted in full.
2. Include an *IMC* Registration Form for everyone seeking support (unless already sent).
3. Include a brief curriculum vitae of everyone seeking support, focusing on aspects relevant to meteor work. Supported participants are expected to present either a talk or a poster at the *IMC*. (Indicate this on the Registration Form.)
4. The application must explain the motivation for attending the *IMC* and the importance of it to the person or group of persons requesting support.
5. Include a budget for travel costs and registration, and the amount of support requested. Other sources of external support, or their absence, must be mentioned. The proposal must indicate to what extent *IMO* support is essential to attend the *IMC*.
6. The applications should reach the President no later than 2005 June 20. The decision of the *IMO* Council will be made as soon as possible, probably within two weeks after this deadline. If the support is granted in full, the registration form becomes final. If the requested support is not granted, or only partially granted, the candidates should inform the President within three weeks after notification of the *IMO* Council's decision if they want to sustain or withdraw their registration. The support granted will be paid in cash at the *IMC*. Any unpaid registration fees will be deducted from the amount paid to the candidates.

Should the application be turned down, the standard conference fee (i.e. €120, without the surcharge for a late application) will still apply. We strongly encourage all meteor workers who want to attend the *IMC* 2005, but who are prevented from doing so by financial considerations, to apply for support.

International Meteor Conference Oostmalle, Belgium, September 15–18, 2005
Registration form

Each individual participant should fill out a form and return it to IMC 2005 — Jan Verbert, Public Observatory Urania, Jozef Mattheessensstraat 60, B-2540 Hove, Belgium, as soon as possible. Your registration will be guaranteed only after Ina Rendtel has received the minimum pre-payment of €60. If you wish to participate, but cannot yet decide, simply return this form with the proper option checked to stay on the mailing list for further circulars.

Name: _____ Date of birth (YYYY-MM-DD): _____

Address: _____

_____

_____

Phone: _____ Fax: _____ E-mail: _____

- I wish to register for the IMC 2005 from September 15 to 18.
- I intend to participate, cannot yet register, but wish to stay on the mailing list.
- I intend to travel by _____, together with _____
- I need travel information from _____ to Oostmalle.
- I wish to stay in Belgium before and/or after the IMC and would like additional information.
- Vegetarian.

T-shirt: Size (S-M-L-XL): _____ Gender: _____

For participants wishing to contribute to the program:
Lecture: _____ Duration: _____ minutes

Workshop or discussion: _____

Poster presentation: _____ Space: _____ m^2

Required equipment: _____

Comments:

Either the entire fee of €120 or a pre-payment of €60 should be sent to IMO treasurer Ina Rendtel. Follow the payment instructions inside the back cover or on the IMC 2005 website `http://wwww.imo.net/imc2005` . Participants making a pre-payment only have to pay the remaining €60 in cash upon arrival in Oostmalle. The registration fee increases to €130 for participants registering after July 1st.

The following payment options are available.

- **International bank transfer** payments should be made to Ina Rendtel, Mehlbeerenweg 5, D-14469 Potsdam, Germany, BIC bank code: PBNKDEFF, IBAN code: DE86 1001 0010 0547 2341 07. When paying, always state BIC bank code and IBAN code together. Always contact your local bank to verify charges for international transfers.
- **German postal giro** Pay in euros to the German postal giro account 547234-107 of Ina Rendtel, Postbank Berlin. Bank code 100 100 10. The bank code and 'Postbank Berlin' should be mentioned together with account number.

Details of the Proceedings of IMC 2004, Varna, Bulgaria

Those who have attended an International Meteor Conference (IMC) will know that they present many high-quality papers on a wide range of meteor subjects. This material is less well known outside the circle of conference-goers, however. To make it more widely available, we are publishing brief details of all IMC 2004 papers here.

Those who attended the Conference will already have received the Proceedings. Others can order them from the IMO: details are in the lower half of the inside back cover of this Journal.

Spectroscopy of the persistent train

Abe, S.

Spectra of persistent meteor trains were observed at wavelength between 300 and 930 nm. Two obtained train spectra during the 1998 and 2001 Leonid meteor showers are reported here. During the 1998 Leonids, one train was detected by a photographic camera with a spectrograph covering 370–640 nm region. On the other hand, during the 2001 Leonids, video observations were carried out using image intensified cameras in ultraviolet, visible and near infrared wavelengths. Temperatures in persistent trains have been measured by atmospheric O_2 A(0,1) band at the wavelength near 864.5 nm. From a video spectrum obtained just 7 seconds after parent fireball's flare, a rotational temperature of 250 K at altitude of 88.0 km was estimated. I can say that the cooling time scale of train strongly depends on the initial mass of its fireball. Based on cooling constant calculated from our results, I estimated a temperature of ∼130 K as a final exothermic temperature at early stage of persistent trains.

Meteor shower analysis exemplified

Arlt, R.

The Visual Meteor Database collects world-wide data of visual meteor observations. The analysis of meteor shower activity is based on computer algorithms. One of them is presented in this workshop with the example of the 2004 Perseids. The algorithm includes adaptive average bins and outlier rejection.

Results of the Perseids–2004

Berinde, Ş., Conu, A. & Grigore, V.

Results of the 2004 summer meteor showers observing campaign of *The Romanian Society for Meteors and Astronomy (SARM)* are presented.

Meteor observations from the Astronomical Observatory at Sliven, Bulgaria

Getsova, I.

A short report about the beginning of our contacts with IMO, and results from our observations of the 2004 Perseids are given.

Ten years of meteor poetry

Gheorghe, A.D.

Parents of meteors (three amusing items from Romania)

Gheorghe, A.D. & McBeath, A.

Observations of the Perseid meteor shower in 1988–2003

Gorjachko, J., Morozov, K., Sergey, I., Bryukhanov, I., Lapitski, Z. & Gain, A.

Tineret Plus-Perseide 2004, an international project in Romania

Grigore, V. & Ogescu, D.M.

It is presented the 12th editions of Perseide (Perseids) manifestation organized by *SARM*, the most important astronomical event in Romania since 1993. Named this year Tineret Plus-Perseide 2004, it had two usually components, the summer astronomical school and the national observing Perseids network and a special tourist program. Over 80 participants attended this event, including observers from the Netherlands, Belgium and Germany.

Meteor phenomenon erroneous related in mass-media

Grigore, V. & Ogescu, D.M.

In this article are shortly presented some aspects of erroneous narration of some astronomical events, especially those related to meteors, which have appeared in the Romanian press and publications during the last few years. We have identified those errors and we suggest some simple measures that can be taken in the near future, in order to counteract this phenomenon.

Perseids 2004 — observations by the MBK Team

Kac, J.

Most of the 2004 Perseid observations were conducted at the YARC 2004 Camp. A declining branch of an elevated activity was observed on 2004 August 11 at $20^{\mathrm{h}}15^{\mathrm{m}}$ UT with a ZHR of 152 ± 7. The highest value of the population index was also reached at about the same time. We used video recordings to derive the Perseid radiant location for the night of the maximum. It is located at $\alpha = 48\overset{\circ}{.}2$ and $\delta = 57\overset{\circ}{.}9$ ($\lambda_{\odot} = 140°$).

The National Astronomical Observatory "Rozhen", Bulgaria — an educational center for young amateur astronomers

Radeva, V. & Stoev, H.

The Bulgarian National Astronomical Observatory "Rozhen" largely contributes to the education of young people in Astronomy. During national and international astronomical summer schools students observe meteors, comets, asteroids, variable stars, and deep sky objects. The results from the observations are presented during regional, national and international conferences. The students are educated by professional or amateur astronomers. Thus, both astronomy and amateur observations are popularized.

Asteroid 2003 EH1 and the Quadrantid meteoroid stream

Ryabova, G. & Nogami, N.

Recently an asteroid 2003EH1 has been discovered on an orbit that is so similar to that of the Quadrantids that some association between them is highly probable. It is also probable that this asteroid and the comet C/1490 Y1 are genetically related. Results of the asteroid's dynamics study is briefly described. Problems arising on study of ancient records of celestial phenomena are shown.

Computer modelling of the June Bootid shower

Shanov, S. & Dubrovski, D.

Some aspects of meteor spectra and their interpretation

Smirnov, V.A.

In this article the characteristics of meteor radiation are investigated. The character of the radiating spectrum depends first of all on the speed of the meteor, and also on the chemical and mechanical structure of the meteoroid. The spectrum of the meteor changes along its atmospheric path according to the Wien's law. For fast meteors the final flares occur due to the particular conditions of the power interaction between the meteoric plasma and particles of the atmosphere. Such features confirm that the meteor plasma can radiate at a speed in excess of 60 km/s in flares, by the mechanism of cascade radiation, which is similar to the radiation of gas-dynamic lasers.

Telescopic meteor observations in Poland

Szaruga, K.

A summary of the 1996–2002 telescopic meteor observations collected by the Polish Comet and Meteor Workshop is presented. Preliminary results of observations of the Perseids, α-Cygnids, o-Draconids, τ-Cepheids and one possible new meteor shower are given. In total, during 997.31 effective hours of observation, 8902 meteors were plotted. All information about the observed meteors has been stored in databases.

June Bootids, radiants from Triangulum, Perseids and δ-Aurigids: three years of video observations

Triglav-Čekada, M., Slavec, S. & Kac, J.

The analysis of 3 years of summer video observations made by Stane Slavec, Astronomical Society Javornik, Slovenia is presented. The data include June, July and August observations from 2002 to 2004. Using the Radiant program the radiants of June Boötids, Perseids and Aurigids are drawn. As a byproduct a meteor shower active in the second half of July in Triangulum is investigated. For the Perseids the population index of video meteors is calculated; radiant drift and possible double structure of radiant is studied. δ-Aurigids or September Perseids are also found to be active in the second half of August.

Short but successful observations of the Geminids in 2003

Velkov, V.

Geminid observations on the night of 2003 December 14/15 by Astroclub Canopus members at Avren Village, Bulgaria, are reported. A maximum in activity was recorded around $21^{\rm h}20^{\rm m}$ UT, $\lambda_\odot = 262\,\overset{\circ}{.}41$, with a great number of bright meteors. An apparent radiant was obtained at $\alpha = 114\,\overset{\circ}{.}5$, $\delta = 32^\circ$.

Observations of the 2004 Perseids from Bulgaria

Velkov, V.

Results are presented of visual and photographic observations of the Perseids carried out by Astroclub "Canopus" in 2004 at three observing sites — Avren Village, the National Astronomical Observatory at Rozhen, and Belite Brezi. Because of the poor weather quantitative ZHR results could not be obtained.

Recent meteor observing activities in Japan

Yamamoto, M.

The meteor train observation (METRO) campaign is described as an example of recent meteor observing activity in Japan. Other topics of meteor observing activities in Japan, including Ham-band radio meteor observation, the "Japan Fireball Network", the automatic video-capture software UFOCapture, and the Astro-classroom programme are also briefly introduced.

Taurids

Radiant ephemeris of the Taurid meteor complex

Mihaela Triglav-Čekada[1] *and Rainer Arlt* [2]

The radiant ephemeris of the Taurid complex meteor showers derived from IMO video observations from 1995–2004 is presented. Detailed radiant ephemerides of the Northern (NPI) and Southern Piscids (SPI) and the Northern (NTA) and Southern Taurids (STA) are derived. Tentative radiant motions of the Northern and Southern χ-Orionids (ORN and ORS) are presented. The Taurids (NTA and STA) are active from the beginning of September to the end of November; the Southern Taurids disappear earlier around November 20. While the Northern Taurids appear to be slower until about October 20 than in the second part of their activity period, the Southern Taurids do not exhibit sub-components. The Southern Piscids (SPI) are active only in September and their activity is much lower than the activity of the Taurids at that time. The Northern Piscids are a little more prominent than the Southern Piscids and are detectable from the beginning of September to October 18, with a probable maximum period from September 20 to October 2.

Received 2005 April 25

1 Introduction

The Taurids are a minor meteor shower active around November and to meteor observers well known by their display of bright fireballs. The fireballs can be seen in greater number in so-called swarm years (Asher, 1994; Arlt, 2000) — the years when Earth encounters the 7/2 resonant Taurid swarm — when Taurids can produce a ZHR of 10 around the maximum. On occasional years the average ZHR does not exceed the background sporadic activity by much, being 5 (Rendtel et al., 1995).

The Taurid complex is also visible in the first part of the year when Earth encounters the meteor stream of the Taurid complex as daytime meteor showers observable only by radio techniques.

The meteor showers of the Taurid complex are connected together by its possible common parent body, the giant comet which disintegrated into smaller ones now known as a family of different comets and asteroids (Asher, 1994). The best known parent body of the Taurid complex is Comet 2P/Encke. Many different Near-Earth Asteroids can also be connected with this complex (Asher, 1994; Klačka, 1995; Babadzhanov, 2001; Porubčan and Kornoš, 2002).

Denning already mentioned the Taurids in his notes in 1883 (Denning, 1883); he mentions very bright and slow meteors radiating from Taurus in November and states in his later publications they are active from August to December (Denning, 1901). Others (Asher, 1994; Babadzhanov, 2001; Porubčan and Kornoš, 2002) distinguish different meteor showers of the Taurid complex, a term referring to showers active over three months. In order of their time of appearance they are: the Southern Arietids, the Southern and Northern Piscids, the Southern and Northern Taurids, and the Northern and Southern χ-Orionids (Asher, 1994). Some authors mention an even more detailed list of meteor showers connected with the Taurid complex, where the aforementioned showers are divided into different meteor streams (Babadzhanov, 2001). Here we will consider just the aforementioned meteor showers, to see if they can be distinguished using the video data.

In a photographic analysis of computed orbits of meteoroids (Steel et al., 1991), the Taurid complex branch with radiants south of the ecliptic is more active than the northern branch. On the other hand, Asher mentions Bone's (1991) research on visual meteors in which the northern branch of Taurids looks stronger. Also, from visual plotted meteors, the southern branch of the Taurids looks stronger (Triglav, 2000). That analysis of 10 years of plotted meteors did not yield a final decision on whether or not visual plottings can distinguish between STA and NTA (Triglav, 1999, 2000).

2 The data set

This radiant investigation of the Taurid meteor shower complex is based on individual meteors recorded by video systems (some image-intensified, some not). All the observations from September to December from 1995 to 2003 placed in the IMO video network database are used (Molau, 2005a,b). The data from 2004 are just a portion of the data published in the IMO video network database home page after 2005 February. The main reason for this is that the analysis began in early December 2004, when only partial 2004 data were available from Sirko Molau. The data prior to 1995 are not used, as no video observations in the period September to December can be found in the IMO video network database. The same is true for the year 1997.

The meteor data of the following observers listed in order of their contribution to the network data is used (Molau, 2005):

> Sirko Molau, Jörg Strunk, Jürgen Rendtel, Orlando Benitez-Sanchez, Steve Quirk, Ilkka Yrjölä, Stane Slavec, Detlef Koschny, Mirko Nitschke, Stephen Evans, Javor Kac, Ulrich Sperberg, Stefan Ueberschaer, Robert McNaught, André Knöfel, Rosta Štork, Michael Gerding.

[1]Streliška 9, SI-1000 Ljubljana, Slovenia
Email: mtriglav@yahoo.com
[2]Friedenstraße 5, D-14109 Berlin, Germany
Email: rarlt@aip.de

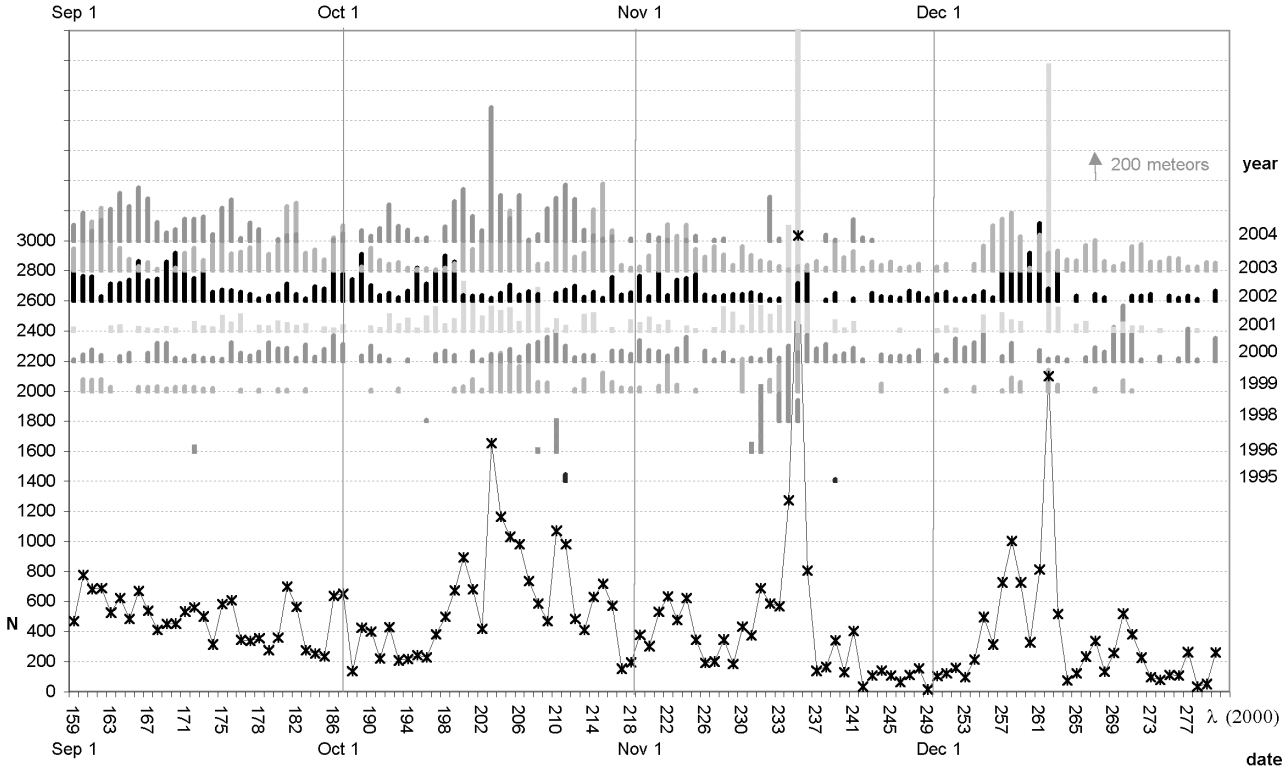

Figure 1 – Video observational statistics. The majority of Leonids are filtered out from the 1995–2003 data (those already classified as Leonids by MetRec); only the 2004 data retain Leonids. The solar longitude is valid for equinox J2000.0, when 1 day is approximately 1° on average in the September – December period. The number of captured meteors in one night per year is presented as a positive error bar. The lowest graph presents the sum (N) of all meteors captured in one night in the period 1995–2004.

These data were all treated as single-station video observations in this analysis. All the meteors were measured using the MetRec software by Molau (1999). The positional accuracy is of the order of few arc minutes. Time differences are known very precisely due to the constant rate of video frames, so the determination of the angular velocity is even more accurate than that of the positions. During computation, the individual meteor positions are projected onto a common (average) plane, and the velocity is computed as the weighted average over all pair-wise distances in this plane. The distance of a part of meteor on a video frame with a larger time difference receives a larger weight, so individual position errors should have little influence on the resulting velocity for meteors captured on a number of video frames (Molau, 2005).

Figure 1 shows the distribution of meteor data by year and date. As mentioned in the caption of Figure 1 the majority of Leonids are already filtered out of the sample, as in this analysis we are not interested in them and because of their overall effect on the number of observed video meteors. When looking at the number of observations per day we made the following conclusions:

- On average at least 100 meteors per day are captured.
- In October, the peaks of the η-Geminids and Orionids stand out from the average.
- In November, despite attempting to filter the Leonids out, they stand out from the average.
- After the Leonid observations there is a void in the number of observed meteors — easily explicable by the 'Leonid leave' as observers had to get back to work or had too much Leonid data reduction work.
- The number of observed meteors rises again with the Geminid display in the first half of December.
- At the end of December observational voids happen again as there are family holidays in the calendar, but this does not affect the Taurid analysis at all.

When looking at the yearly distribution of the video observations, we can make a separate yearly analysis of the Taurids just for the years 2000–2004. Prior to those years there is too little data to make any usable conclusions.

Altogether this data sample consists of 57 778 meteors. Once more we have to emphasise that the majority of Leonids are filtered out, which means that this data sample is not dominated by them. Table 1 presents the number of meteors captured in this time interval in one year.

3 Method

The radiant analysis presented in this paper was made with the Radiant program by Arlt (1992, 2001). All the radiant plots are the result of the 'Probability functions' of the Radiant software. 'Probability functions'

Table 1 – The observational statistics by year.

Year	1995	1996	1998	1999	2000	2001	2002	2003	2004	sum
N	52	709	740	3958	6934	9765	11015	16187	8418	57 778

are more powerful representations of the radiant than simple backward prolongations of the meteor. If path and velocity are precisely known, each individual meteor has one point (actually two on a great circle in general) which is its radiant. Plotting errors and uncertainties in the speed estimate smear this point into an area of varying probability of being the radiant of that meteor. The values in this probability area form a sort of two-dimensional Gaussian function (Arlt, 1992, 2001, 2003). For more detailed information about the 'probability functions' see (Arlt, 2003).

Unless otherwise stated, the parameters used in this analysis to construct the 'probability functions' are shown in Table 2.

4 Investigated Taurid Complex meteor showers

4.1 Northern and Southern Taurids

The Northern and Southern Taurids are the best known and the most active part of the meteor showers comprising the Taurid complex. The working list of visual meteor showers in (Rendtel et al., 1995) states the activity period of both showers (NTA and STA) to be from October 1 to November 25. The intention in that list was to split the ecliptical meteor activity into adjacent periods of individual shower designations. For example, the Southern Piscid radiant as the predecessor of STA was listed for September 1–30. The NTA have a velocity of $v_\infty = 27$ km/s, the STA $v_\infty = 29$ km/s. A rough search in the IAU database of meteoroid orbits delivered a median velocity of 30 km/s for NTA and 29 km/s for STA from samples of 64 and 60 orbits respectively. The differences are in fact all within the typical scatter of ecliptical meteoroid orbits.

4.2 Northern and Southern Piscids

The Piscids are an even weaker meteor shower than the Taurids. In (Rendtel et al., 1995) only the Southern Piscids are mentioned with $v_\infty = 26$ km/s and a ZHR of 3 around the maximum on September 20 ($\lambda_\odot = 177°$). As already mentioned, they are listed for September 1 to September 30. Detailed analysis of IMO visual observations by Dubietis (2001) finds a broad maximum between September 18 and September 21 for the SPI activity.

The Northern Piscids were considered to have even lower activity and were therefore not mentioned in the working list for visual observers (Rendtel et al., 1995). The previous working list mentioned the shower as being active from September 25 to October 19 with a maximum on October 12 and $v_\infty = 29$ km/s. Cannon's (2001) collection of meteor showers from different lists states their activity as from August 12 to October 12, with a maximum also (anomalously) on October 12 and with no hint about their velocity.

It is not quite clear whether the Piscids show a distinct separation into northern and southern branch as the Taurids do. We will later show that they are distinct but much less obviously so than the Taurids.

While the velocities of NPI and SPI are 29 and 26 km/s, respectively, the NTA and STA velocities are just vice versa. Again we have to bear in mind that the scatter of velocities among ecliptical meteoroids is large, and the values quoted may be affected by too small orbit samples. The median velocities may in fact all be very similar.

Babadzhanov (2001) mentions other Piscids with smaller velocities: the Northern October Piscids with an observed radiant on October 25 ($\lambda_\odot = 211\overset{\circ}{.}8$) at $\alpha = 16\overset{\circ}{.}2$ and $\delta = 14\overset{\circ}{.}6$ with $v_\infty = 17.5$ km/s, and the Southern October Piscids with dates for October 24 ($\lambda_\odot = 210\overset{\circ}{.}8$) at $\alpha = 23\overset{\circ}{.}2$ and $\delta = 7\overset{\circ}{.}2$ with $v_\infty = 19.2$ km/s. The lower velocity is due to the fact that the radiant lies farther from the apex of the Earth's motion.

4.3 Different χ-Orionid meteor showers

The χ-Orionids (XOR) are a very weak meteor shower listed as being active from November 26 to December 15, with a maximum on December 2 ($\lambda_\odot = 250°$). Again, the activity period is meant to be complementary to the Taurids, ending on November 25 by the working list definition. The XOR is expected to exhibit a very big radiant area for visual observers. Their velocity is $v_\infty = 30$ km/s (Rendtel et al., 1995). Some authors divide them in northern and southern branch.

5 Radiant drift of Taurids at daily intervals

The daily radiant drift of the Taurids was calculated for intervals of one degree in solar longitude ($200\overset{\circ}{.}37 < \lambda_\odot < 201\overset{\circ}{.}37$, $201\overset{\circ}{.}37 < \lambda_\odot < 202\overset{\circ}{.}37$, $202\overset{\circ}{.}37 < \lambda_\odot < 203\overset{\circ}{.}37$, etc.) which is approximately a one-day interval. For the center of the calculation the midnight of the relevant day's solar longitude for the year 2000 was used (J2000). The pixel size of the computational grid was set to $0\overset{\circ}{.}3$ so an area of approximately $30° \times 30°$ was covered when computing the radiant, and the maximum allowed distance of meteors from the center of that grid was set to 70°. For each Taurid branch a separate calculation was made by changing v_∞: 27 km/s was used for NTA and 29 km/s for STA as mentioned in (Rendtel et al., 1995).

The errors given as 'err' in Table 12 (page 58) are 68% confidence intervals around the point of maximum probability. Actually these confidence intervals are measured in α and δ directions independently, and the larger of the two is given in the Table. Both equatorial coordinates and ecliptical coordinates of the radiants are measured. Note that these errors do not include positional changes introduced by the uncertainty of parameters such as velocity, which was held constant here.

Table 2 – Values for the angular velocity and plotting standard deviations of video observations as used in Radiant (Arlt, 2003). Values in between the distances and velocities listed were obtained by linear interpolation.

Distance d	0°	5°	15°	30°	50°	70°	
$\sigma(d)$	0.5°	0.9°	1.3°	1.5°	1.7°	1.8°	
Velocity ω	2.5	7.5	12.5	17.5	22.5	27.5	>30
$\sigma(\omega)$	1.0	1.5	1.9	2.3	2.6	2.9	3.0

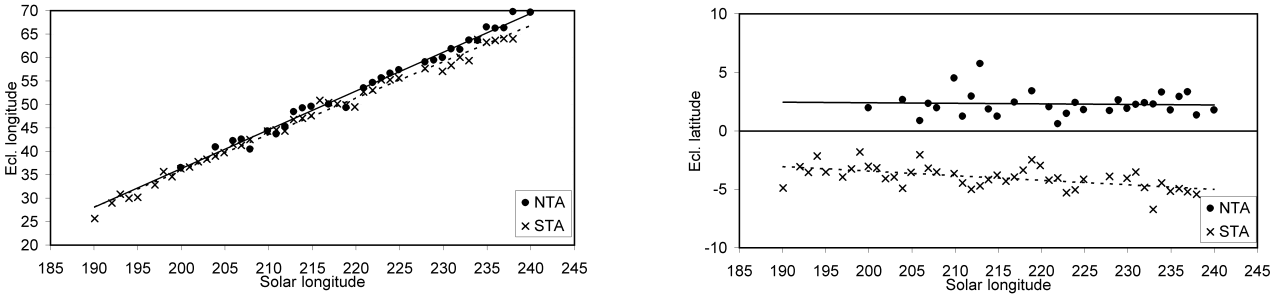

Figure 2 – Left: the progression of ecliptical longitude (l) and right: the progression of ecliptical latitude (b) of the NTA and STA.

Table 12 also gives the number of selected meteors N in each one-degree solar longitude interval; $n_{\min}$ is the number of meteors contributing to the 30° × 30° window and is the minimum number from computations at $v_\infty = 27$ km/s (NTA) and $v_\infty = 29$ km/s (STA). The highest values differ from $n_{\min}$ by one or a few meteors. We must point out that the number of meteors used for the calculation of the radiant includes Taurids and possibly some sporadic meteors; in the beginning and end of the season, different ecliptical showers from same area are also included.

The radiant positions from Table 12 were used for the computation of radiant drift. The dates marked '*' were not used for the calculation of the regression line for the radiant drift, as these radiant displays were made using less than 50 meteors. In these cases the radiant positions derived are doubtful, and the measured values are not included in the table. The dates marked '**' indicate the days when more than one radiant at the predicted position of STA or NTA can be found — those results are also doubtful and are therefore not used in the calculation of radiant drift. Not the whole period of Taurid activity is covered in this table and the radiant drift computation. We did not use the beginning and end periods of both showers as there are some other radiants which interfere with Taurids and thus it is hard to distinguish them on the basis of one degree solar longitude periods. We will check those intervals in more detail later.

The regression through the points from $\lambda_\odot = 190\overset{\circ}{.}0$ to $\lambda_\odot = 240\overset{\circ}{.}0$ leads to an ecliptical coordinate drift written for a day of a maximum (see Figure 2) of

$$l = 61.16^\circ + (\lambda_\odot - 230^\circ) \cdot 0.83, \quad (1)$$
$$b = 2.27^\circ - (\lambda_\odot - 230^\circ) \cdot 0.005 \quad (2)$$

for NTA and

$$l = 53.66^\circ + (\lambda_\odot - 223^\circ) \cdot 0.78, \quad (3)$$
$$b = -4.33^\circ - (\lambda_\odot - 223^\circ) \cdot 0.039 \quad (4)$$

for STA.

If we combine all measurements of ecliptical longitude for the NTA and STA and just draw a common regression line, we get the overall radiant drift by the ecliptic of $\Delta l = 0\overset{\circ}{.}81$ for 1° solar longitude interval. That means that for the interval from October 3 to November 22, 1 day is about 1° of solar longitude on average, and that the common radiant drift is also $0\overset{\circ}{.}81$ per a day interval. We will use this radiant drift in the following calculations.

The corresponding regression lines through the equatorial coordinates deliver

$$\alpha = 58.43^\circ + (\lambda_\odot - 230^\circ) \cdot 0.86, \quad (5)$$
$$\delta = 22.50^\circ - (\lambda_\odot - 230^\circ) \cdot 0.20 \quad (6)$$
$$(7)$$

for NTA, and for STA

$$\alpha = 33.57^\circ + (\lambda_\odot - 223^\circ) \cdot 0.77, \quad (8)$$
$$\delta = 14.30^\circ - (\lambda_\odot - 223^\circ) \cdot 0.18. \quad (9)$$

The expected radiant motion is parallel to the ecliptic, however, and it should be kept in mind that a linear representation of the drift in equatorial coordinates is of limited use. We have nevertheless given them here in order to allow a comparison with other authors.

When doing one-degree solar longitude calculations, the NTA can be clearly distinguished only from October 16 ($\lambda_\odot = 203°$) onwards. At the end of Taurid activity the STA branch disappears on November 20 ($\lambda_\odot = 238°$). The NTA stays there for a couple of days longer.

Table 3 – Comparison of Northern and Southern Taurid radiant drifts by different authors.

Author	NTA	
Porubčan and Kornoš (2002)	$l = 53.61° + 0.7600° \cdot \lambda_\odot$ $\alpha = 58.6° + (\lambda_\odot - 220°) \cdot 0.80°$	$b = 2.71° - 0.0136° \cdot \lambda_\odot$ $\delta = 21.60° - (\lambda_\odot - 220°) \cdot 0.16°$
Rendtel et al. (1995)	$\alpha = 58° + (\lambda_\odot - 230°) \cdot 0.76°$	$\delta = 22° - (\lambda_\odot - 230°) \cdot 0.10°$
This paper	$l = 61.16° + (\lambda_\odot - 230°) \cdot 0.83°$ $\alpha = 58.43° + (\lambda_\odot - 230°) \cdot 0.86°$	$b = 2.27° - (\lambda_\odot - 230°) \cdot 0.005°$ $\delta = 22.50° - (\lambda_\odot - 230°) \cdot 0.20°$

Author	STA	
Porubčan and Kornoš (2002)	$l = 51.89° + 0.7444° \cdot \lambda_\odot$ $\alpha = 48.7° + (\lambda_\odot - 220°) \cdot 0.73°$	$b = -4.72° - 0.0233° \cdot \lambda_\odot$ $\delta = 13.0° - (\lambda_\odot - 220°) \cdot 0.18°$
Rendtel et al. (1995)	$\alpha = 50° + (\lambda_\odot - 223°) \cdot 0.79°$	$\delta = 13° - (\lambda_\odot - 223°) \cdot 0.15°$
This paper	$l = 53.66° + (\lambda_\odot - 223°) \cdot 0.78°$ $\alpha = 33.57° + (\lambda_\odot - 223°) \cdot 0.77°$	$b = -4.33° - (\lambda_\odot - 223°) \cdot 0.039°$ $\delta = 14.30° - (\lambda_\odot - 223°) \cdot 0.18°$

5.1 Comparison with other authors

Porubčan and Kornoš (2002) computed the radiant drift from photographic Taurids which were also used for Taurid stream orbit calculations. Due to very long duration of the stream activity, the motion of the shower radiant in equatorial coordinates cannot be treated as linear. Thus the radiant drift for α and δ mentioned it that paper is valid only for an interval around $\lambda_\odot = 220°$ and is comparable with our calculations.

We find a radiant drift also in (Rendtel et al., 1995) but only for equatorial coordinates.

The general tendency in radiant drift in l is the same for video and photographic observations. In (Porubčan & Kornoš, 2002) the values of radiant drift are a little bit smaller, on average $0\overset{\circ}{.}75$ in l, whereas we derived $0\overset{\circ}{.}81°$ on average. When we compare equatorial coordinates we can say our results fit in nicely with values from Porubčan & Kornoš (2002) and Rendtel et al. (1995).

6 Taurid complex radiants ephemerides for 5°-solar longitude periods

With the radiant drift of $0\overset{\circ}{.}81$ computed above we made a second computation of radiant positions for 5°-solar longitude periods, which corresponds approximately to a 5-day period.

For this computation the number of selected meteors N is much higher than before, so we just used meteors to a maximum distance of 50°, though at intervals with fewer meteors we also used a maximum distance of 70°. Also different velocities were used (v_∞ = 21, 23, 25, 27, 28, 29, 33 and 37 km/s) to distinguish between different radiants. This was very useful at the beginning and end of the Taurid activity: it indicated from which other showers the ecliptical sources possibly evolve into the Taurids, and into which it possibly evolves at the end. At the beginning there were Piscids and at the end χ-Orionids.

The timetable of the calculation was: first October and November when the Taurids are highly active, then checking back in time in September, and finally also the beginning of December. Checking if more detail can be seen in September calculations reduced the velocity errors mentioned in Table 2. The error used for a velocity of 2.5°/s was 1.0°/s, for 7.5°/s was 1.1°/s, ... and for > 30°/s it was 1.6°/s. The result of this test did not give any better details of the radiants; nor was any difference in radiant position seen, just a reduction in the number of meteors used in the calculation of the radiant. This means that fewer meteors were defined as possible radiant contributors.

At the same time the calculations for different magnitude ranges were done for 5°-solar longitude intervals at v_∞ = 28 km/s (and 21 km/s just for September). As mentioned in (Arlt, 2003), we divided our data in three magnitude ranges: bright meteors ($m < +1.0$), average meteors ($+1.0 \leq m < +2.7$), and faint meteors ($m \geq +2.7$). With this check we can find out if any meteor shower is more prominent in one specific magnitude range. This would suggest defining a shower as mostly seen telescopically if its meteors produced a radiant only in the faint meteor range. Alternatively, for a meteor shower just seen in the bright magnitude range, this would be a fireball source. Meteor showers seen in all three ranges would present typical meteor showers equally prominent in all magnitude ranges.

6.1 September

According to the plots in Figure 3, northern and southern ecliptical sources are found for September. It is very difficult to say whether Piscids and Taurids are two dis-

Table 4 – Data for Figure 3 — the September radiant plots. N is the total number of meteors from that interval, n is the number of meteors actually contributing to the radiant plot.

Date	$\lambda_\odot$ [°]	v_∞ [km/s]	N	n	
Sept 05	162.74	29	3109	316	
Sept 10	167.59	29	2753	274	
Sept 15	172.33	29	2624	244	
Sept 20	177.33	29	2231	279	
Sept 25	182.22	29	2180	274	
Sept 30	187.13	28	975	111	*

* Middle magnitude range

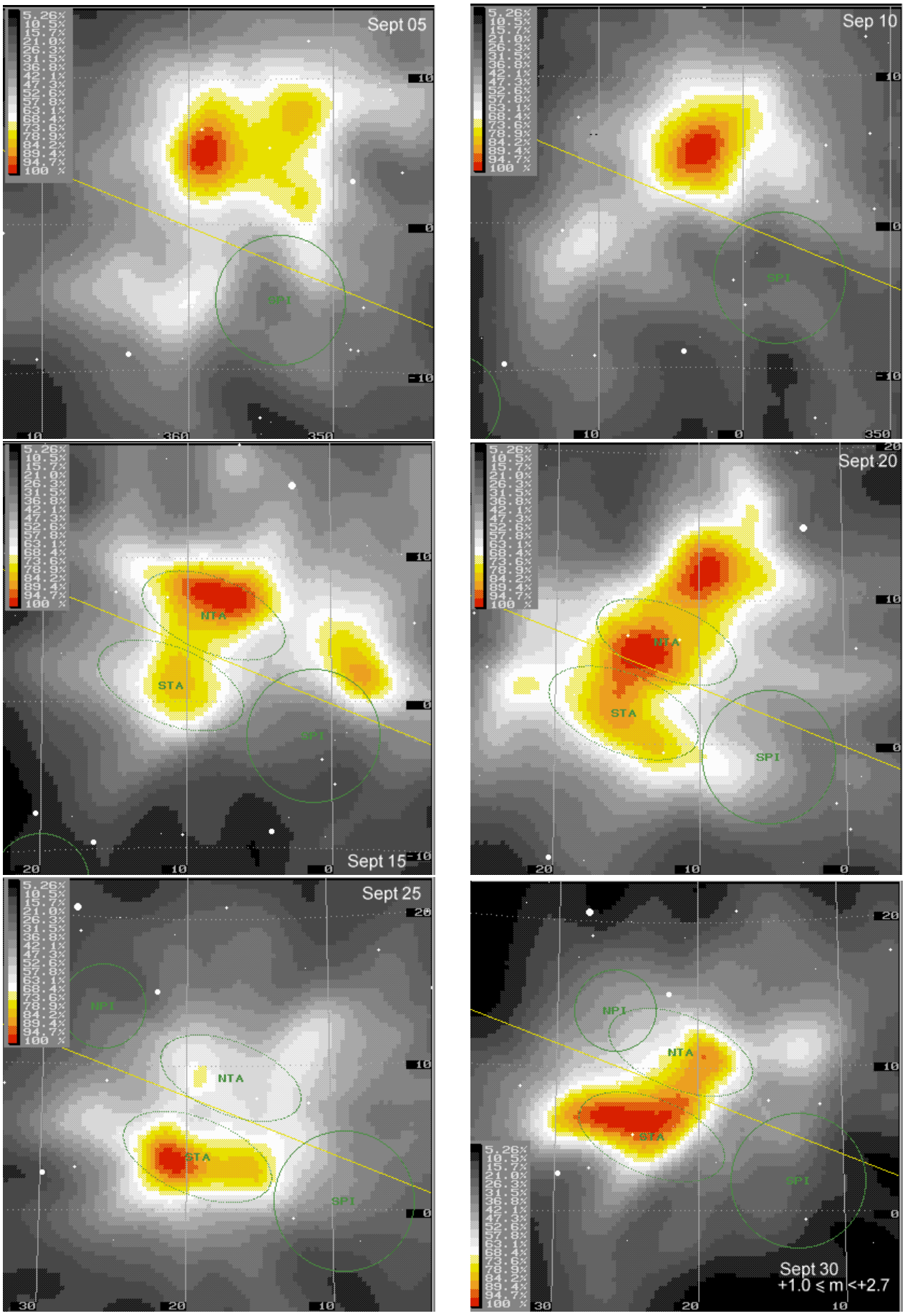

Figure 3 – September radiant plots.

tinct sources, because east-west separation is only visible clearly in the September 15 display.

The velocity on which the radiant computations are based has a two-fold effect. On the one hand, those showers should appear with their best prominence if the computational velocity matches the true velocity. On the other hand, the distribution of meteors around our region of interest is not isotropic. The vast majority of meteors recorded lie *north* of the radiant search area. Let us for the moment consider a single meteor north of this region. At a given observed angular speed, the probable radiant lies close to the meteor if one assumes a high pre-atmospheric velocity. If one assumes a small velocity, the observed angular speed matches a radiant farther away from the meteor, i.e. farther south. Now the accumulated distribution of radiants of all the meteors — chiefly positioned north of our region of interest — will shift in the same manner when varying the pre-atmospheric velocity.

This is why the most prominent radiants south of the ecliptic are seen at smaller velocities v_∞=20–29 km/s. The NTA at $\alpha = 14°$, $\delta = 6°$ are thus best seen at higher velocities (29, 33, 37 km/s). On September 15, a separate NPI radiant may be spotted a little further north of the NTA radiant. The NPI radiant is also best seen at higher velocities (26–40 km/s), and is placed at $\alpha = 9°$, $\delta = 13°$. At the shower list position of the SPI, very little indication for a radiation area is found: according to Figure 3 (September 20) only as an outgrowth from the STA radiant.

These four radiants can be seen even when we check different magnitude ranges.

- It seems that the SPI together with the STA are the most active in the range of faint meteors, as then the radiants are combined into one big elongated radiant which dominates in the southern part of ecliptic.
- The SPI and STA radiants can be nicely divided into two radiants in the middle magnitude range, when SPI are the weakest.
- In the bright magnitude range we can see only the NPI in the north and the STA in the south, but these are inconclusive results as only 37 meteors out of 517 were used for the calculation.

Before that, on September 15 three radiants are visible: NTA, STA and NPI. The NTA stand at $\alpha = 8°$, $\delta = 8°$ and the STA at $\alpha = 10°$, $\delta = 1°$. They are both equally prominent at v_∞=26 km/s. In the north the NPI radiant also stands at $\alpha = 358°$, $\delta = 2°$ with a lot of bright meteors — only this radiant is seen in the bright magnitude range. For this analysis, 29 meteors were selected from the database for the studied period; 631 meteors contributed to the radiation area distribution in the field of computation. (Henceforth, notations like (29/631) will be used to indicate these numbers.) When comparing different velocities, the NTA radiant seems the most prominent at higher velocities at this time. There is no sign of an SPI radiant. In the middle magnitude range, the NTA and SPI radiants are seen best. In weak magnitude range the STA radiant is very prominent — this means that the STA at this time comprise mainly weak meteors.

If we check them even further back, we can see on September 10 that the NTA have the most prominent radiant at the location $\alpha = 4°$, $\delta = 5°$. The STA are less prominent and lie at $\alpha = 10°$, $\delta = -2°$; they comprise mainly middle and weak magnitude range meteors. In the north the NPI are hardly seen, just as an outgrowth from the NTA at $\alpha = 358°$, $\delta = 5°$. We can only distinguish the NPI clearly in the bright magnitude range, but the radiant plot was made from 50 meteors out of a total of 688. At smaller velocities even a very vague (40 % probability) SPI radiant can be seen at $\alpha = 357°$, $\delta = -5°$.

Even 5 solar degrees earlier, on September 5, the state is similar with the difference that three radiants seem to be active in the north. The NPI are the most prominent at higher velocities at $\alpha = 353°$, $\delta = 2°$. The NTA are best seen at the higher velocities at $\alpha = 358°$, $\delta = 5°$. The third north unknown radiant lies at $\alpha = 353°$, $\delta = 7°$. The SPI are almost doubtful as the radiant moves around when the velocity is changed from 24 to 33 km/s. They can only be positioned on the same spot when comparing the velocities 21 and 24 km/s, but this is too small so we will not report its position. On the plot for smaller velocities the STA stand out nicely at $\alpha = 353°$, $\delta = -7°$. In the middle and weak magnitude ranges, the most prominent radiant is the NPI. In the bright magnitude range the STA radiant is seen clearly (42/717).

Returning to the main topic, we consider what is happening at the end of September: again we can distinguish all four radiants on September 25. The Taurid couple is closer together and near the ecliptic with the NTA at $\alpha = 19°$, $\delta = 9°$ and the STA at $\alpha = 22°$, $\delta = 3°$. At this time the Taurids form more compact and prominent radiants than the Piscids, and this is especially true for the STA. At this time we can also say the southern radiants come out from behind the prominence of the northern couples. The Piscid radiants lie further apart, divided by the ecliptic, and are also more dispersed and less prominent. The more prominent and compact SPI radiant lies at $\alpha = 16°$, $\delta = 3°$, and the NPI can be placed at $\alpha = 13°$, $\delta = 8°$. In the middle magnitude range the NPI divide into two radiants, one over the other, and only the northernmost one remains evident in the weak magnitude range. The SPI and STA are also divided in the middle magnitude range, the STA being clearly more prominent. The bright magnitude range has too few meteors used in computation so no conclusions can be drawn from it (34/451).

On September 30 it seems that the STA and SPI pour into one big and very prominent radiant which shows little change when varying the velocity v_∞ from 24 to 29 km/s. They stand out at $\alpha = 24°$, $\delta = 7°$ with a radius of approximately 4°. It appears that the STA are positioned within this overall radiant at more like $\alpha = 26°$, $\delta = 8°$, as they are still visible at $v_\infty = 33$ km/s. In the north part of ecliptic the NTA get a new spring into their activity, so at this time they dominate

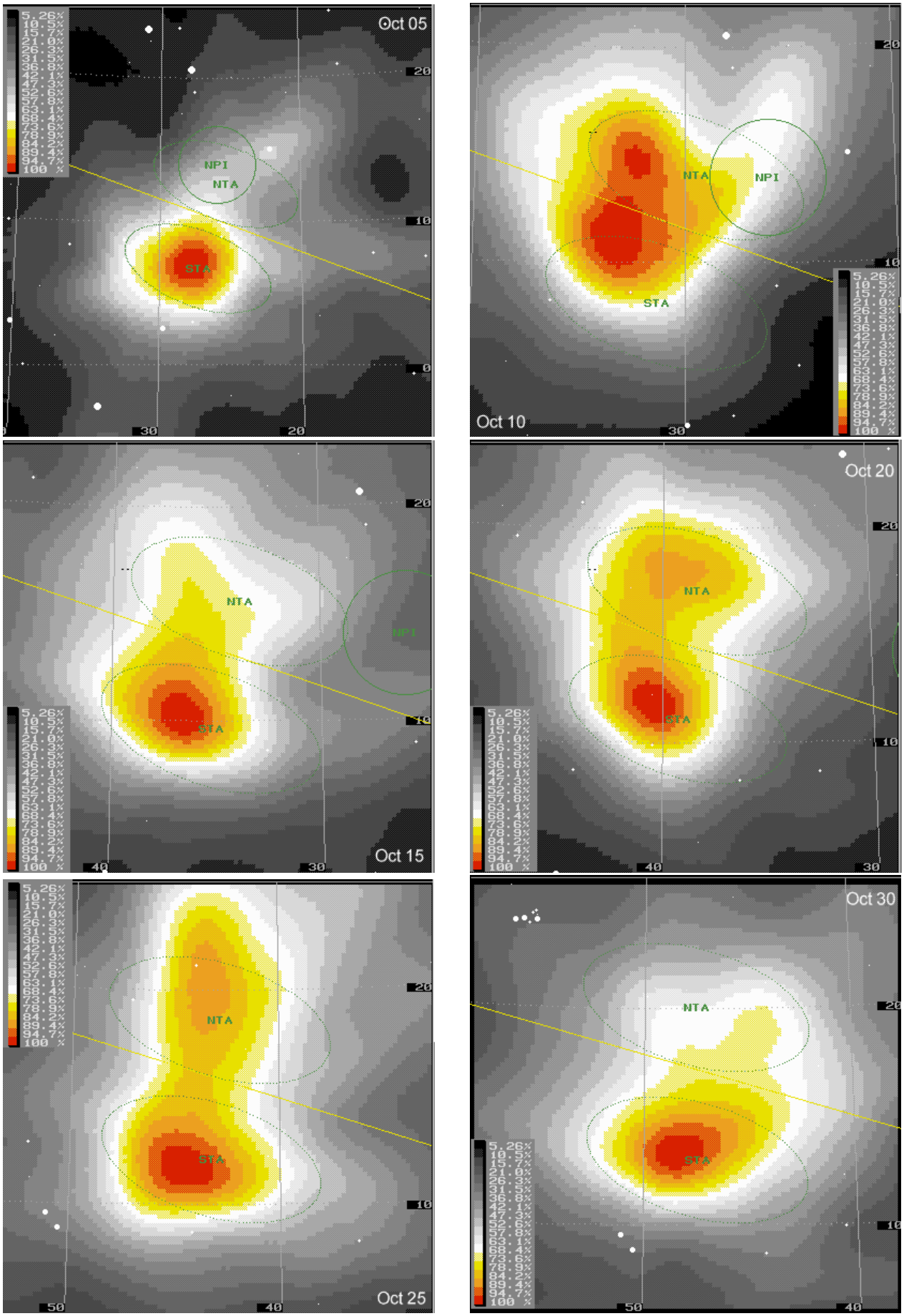

Figure 4 – October radiant plots.

and are placed at $\alpha = 20°$, $\delta = 11°$. The NPI radiant cannot be distinguished from the overall data as they present just a little outgrowth from the NTA radiant to the right. However, we can clearly see them as a separate radiant in the bright and middle magnitude ranges at $\alpha = 13°$, $\delta = 11°$. The NPI disappear in the weak magnitude range.

6.2 October

In the next interval on October 5, in the south only the STA remain easy visible at all velocities checked (from 24 to 33 km/s). This radiant is placed at $\alpha = 28°$, $\delta = 7°$. It is still the most active source in this period. The NTA are still a hard to distinguish outgrowth from the southern components; maybe the activity of this component of the NTA notable at higher velocities has ended. The NPI are moving more to the north from the ecliptic and are becoming more dispersed at $\alpha = 22°$, $\delta = 15°$. In this period there are too few bright (45/405) and middle (59/652) magnitude range meteors contributing to those radiants, so we can say the majority of Taurid and Piscid meteors in this period are weak.

On October 10, the STA is again the most powerful source in this part of the sky, placed at $\alpha = 32°$, $\delta = 9°$. The NTA and NPI can only be distinguished from that big and prominent southern radiant if we check the area at higher velocities. The interval has a slightly non-uniform distribution of meteors contributing to the radiant plot, as all meteors have been observed only on the north side of Taurid radiants; this can explain why the increase in velocity causes radiants to shift to the north. The NTA radiant is clearly visible only at $v_\infty = 33$ km/s and $\alpha = 32°$, $\delta = 14°$. The NPI are again the same as in previous interval, so we can only see a hint of them somewhere at approximately $\alpha = 29°$, $\delta = 12°$. The radiant plots at different magnitude ranges show no difference where the STA radiant is concerned. There is only a slightly greater hint of the NPI as an outgrowth from STA radiant in the middle magnitude range.

The northern branches are again very vague on October 15. We can say the NPI radiant is disappearing and the NTA has not became very active yet. Both radiants present a weak outgrowth a little more prominent at higher velocities. This time the meteors are approximately evenly distributed around the radiants (2/3 to the north and 1/3 to the south). We can place the NTA somewhere about $\alpha = 36°$, $\delta = 15°$. In the south, only the STA is seen equally for different velocities at $\alpha = 37°$, $\delta = 10°$. The NTA stand out at the brighter magnitude range as a separate radiant (137/1690); at the middle magnitude range they are a very powerful outgrowth from STA, but in both cases they are still very weak compared with the STA radiant.

Again on October 20, the STA are equally prominent for velocities from 23 to 33 km/s at $\alpha = 40°$, $\delta = 12°$. On the northern side, only a big NTA can be extracted out of the surroundings as a separate radiant at higher velocities (30 and 33 km/s). The NPI are no longer visible. It is interesting that the NTA radiant for bright meteors lies four degrees east of the radiant of the faint NTAs. The positions are $\alpha = 39°$, $\delta = 18°$ (89/995) for the bright and $\alpha = 35°$, $\delta = 16°$ (176/1249) for the faint component. There is no sign of either radiant in the middle magnitude range if computed with $v_\infty = 28$ km/s.

The STA still dominate the radiant display on October 25. They can be seen at all velocities at $\alpha = 44°$, $\delta = 12°$. On the north side of the ecliptic one common radiant is placed at $\alpha = 43°$, $\delta = 19°$. The NTA are becoming more active, as the northern radiant can be distinguished even at a velocity of $v_\infty = 21$ km/s. Sub-components of the NTA cannot be separated into two radiants as in the previous interval. In the bright magnitude range (68/946), we can see the NTA radiant around 3° more to the west than that from the middle magnitude range (139/1518). This is the opposite of what we observed in the October 20 plots, and the main conclusion we can draw is that the Taurid radiants are not very confined and stable structures, but indeed more diffuse regions with a variability of 1°–2° in position than the radiants of the Perseids or Leonids, for example.

On October 30 the STA is placed at $\alpha = 48°$, $\delta = 14°$. The NTA radiant presents an outgrowth from the STA radiant at $v_\infty = 26$ and 29 km/s. It is nicely visible in the middle (112/842) and weak (148/801) magnitude ranges at $\alpha = 46°$, $\delta = 18°$ as a middle-prominence radiant still connected to the southern radiant. The bright magnitude range comprised too few meteors (55/566), therefore no conclusions can be drawn from it.

Table 5 – Data for Figure 4 — the October radiant plots. N is the number of all meteors from that interval, n is the number of meteors actually contributing to the radiant plot.

Date	$\lambda_\odot$ [°]	v_∞ [km/s]	N	n	
Oct 05	192.06	27	1499	221	
Oct 10	196.99	33	1888	265	
Oct 15	201.94	33	4907	495	
Oct 20	206.90	33	3652	375	
Oct 25	211.88	30	3966	371	
Oct 30	216.87	30	2209	283	*

* $\Delta\lambda_\odot = 6°$

Table 6 – Data for Figure 5 — the November radiant plots. N is the number of all meteors from that interval, n is the number of meteors actually contributing to the radiant plot.

Date	$\lambda_\odot$ [°]	v_∞ [km/s]	N	n	
Nov 05	222.88	27	2646	527	
Nov 10	227.89	25	1349	301	
Nov 15	232.92	25	3019	653	
Nov 20	237.97	28	1542	281	*
Nov 25	243.02	31	850	167	
Nov 30	248.08	31	596	100	

* Faint magnitude range

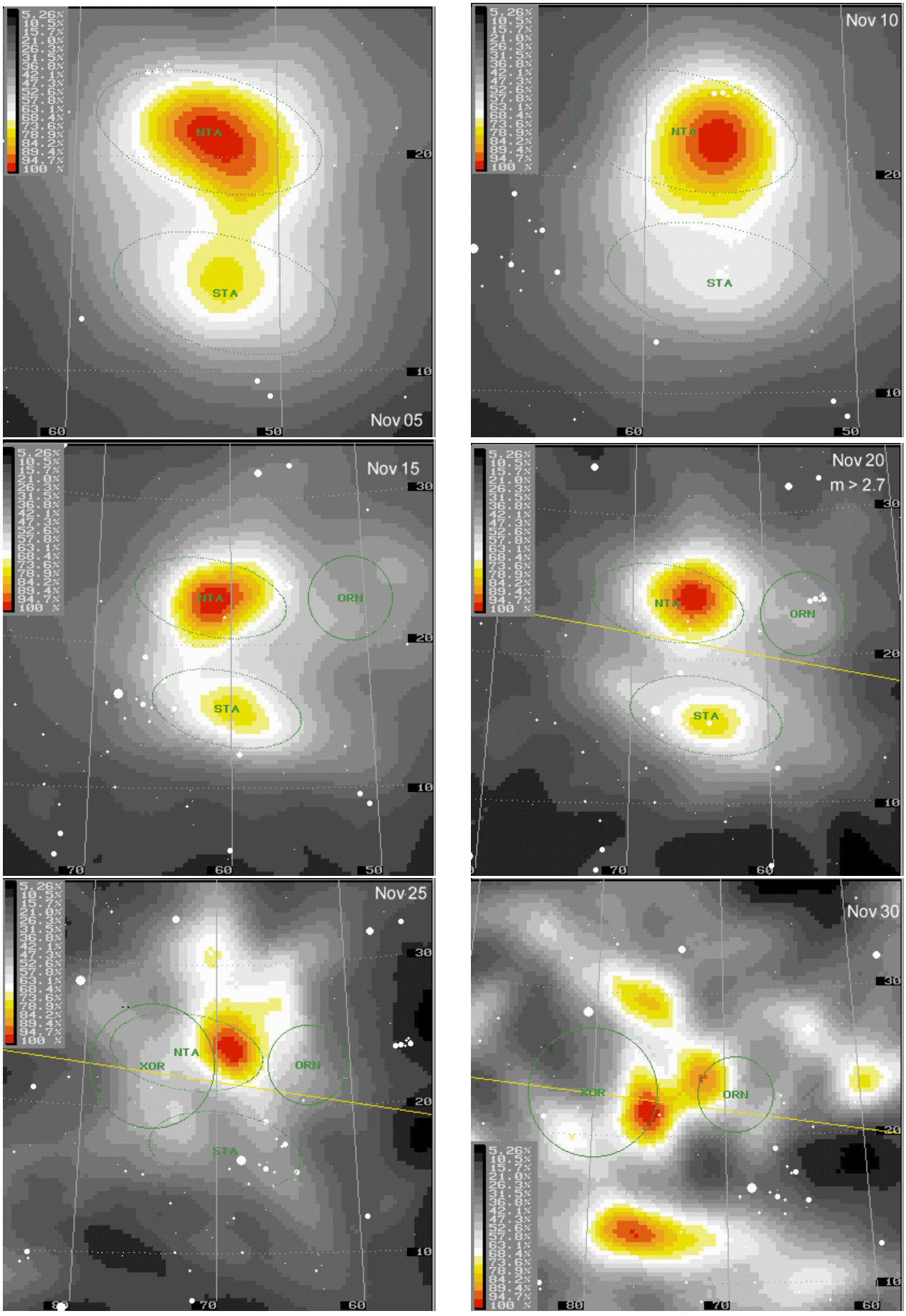

Figure 5 – November radiant plots.

6.3 November

Here it must be noted that as a byproduct of Leonid observations in November (see Figure 1), we get a much better distribution of meteors around listed radiants until the lack of observations at the end of November. This means that our conclusions on the positions of radiants are more certain for this month.

November is the month of greatest NTA activity. Their prominence already exceeds their southern partner on November 5. The NTA radiant stands at $\alpha = 53°$, $\delta = 21°$. The STA are at $\alpha = 53°$, $\delta = 15°$ and are strongest for the faint meteor class.

On November 10, the STA become less prominent compared to previous intervals, they lie at $\alpha = 57°$, $\delta = 16°$. This means that at this time the NTA outnumber them greatly. The NTA are positioned at $\alpha = 56°$, $\delta = 22°$ and are seen at all velocities. The STA radiant can be extracted as a separate radiant only in the weak magnitude range. In the middle magnitude range they present a clear extension of the NTA radiant.

In the next interval on November 15 both radiants are seen well. The NTA are still more active and have their radiant at $\alpha = 61°$, $\delta = 23°$. The STA radiant is at $\alpha = 60°$, $\delta = 16°$. This is the first period when the meteors are distributed more isotropically around the center of the computational area. Changing the velocity on which the radiant computation is based results in much smaller 'radiant drifts'.

When comparing the behavior of the radiants in different magnitude ranges, the STA prominence becomes comparable to NTA prominence only in the weak magnitude range, meaning that the STA are again composed mainly of faint meteors. At this time, west of the NTA, a radiant which can be associated with a northern branch (ORN) of the χ-Orionids (XOR) becomes barely visible. We can locate it at $\alpha = 48°$, $\delta = 25°$. It is more prominent at smaller velocities and for faint meteors.

On November 20, the possible ORN are still barely detectable in the faint magnitude range at $\alpha = 57°$, $\delta = 23°$. They are not seen on the plots for all magnitudes; they are probably exceeded too much by the NTA radiant. The NTA are at this time still the most active source at $\alpha = 66°$, $\delta = 24°$, but the STA at $\alpha = 65°$, $\delta = 16°$ are also a distinct source with next to no deviation from the shower-list position. Both radiants can be seen for different velocities from 25 to 30 km/s with very clear positions as the meteor distribution is now very isotropic. The STA radiant is more elongated, particularly in the middle magnitude range, while the NTA radiant is fairly circular.

On November 25 the STA radiant suddenly vanishes almost entirely. We can see a weak radiant on the southern side of the ecliptic (see Figure 5, November 25) for the velocities 21–31 km/s at $\alpha = 57°$, $\delta = 23°$. The most prominent radiant at this time is still the NTA radiant at $\alpha = 69°$, $\delta = 24°$. As we had only 850 meteors to hand for a full calculation of this interval, the different magnitude ranges are composed of too few meteors to deliver individual radiant distributions.

Another interval with poor observing results is November 30, with only 596 meteors in this interval (see Figure 1 for more detail). Near 30 km/s, an ecliptic source is the strongest for this period. While this source moves south if the velocity decreases, we have to associate this with the meteor distribution effect rather than with a real southern component. All meteors contributing to the displays appeared north of the computational area. The position of this source is $\alpha = 76°$, $\delta = 22°$. Further to the west is a possible ORN radiant at $\alpha = 71°$, $\delta = 24°$. On the south side of the ecliptic, the Southern χ-Orionids (ORS) may become active in this interval and are positioned at $\alpha = 76°$, $\delta = 14°$.

After November 25, the picture is dominated by radiation areas which show little stability when parameters change. The difference from the earlier November and October pictures shows how distinct a source the Taurid couple is compared to the ecliptical background activity at other times of the year.

6.4 The first part of December

In the first part of December, the ecliptical sources are still split north-south as can be seen in the top panel of Figure 8 (page 53). The transition from the radiant positions at the end of November to the December 5 plot is smooth. There is no clear break of a new shower starting, but we prefer to call the December ecliptical radiants χ-Orionids. They have been called XOR collectively in the IMO Working List, but here we use the split designations ORN and ORS for northern and southern components, respectively.

These radiants are in the vicinity of the powerful Geminid radiant which dominates the radiant displays of the 5-day periods around December 10 and 15. We can see the χ-Orionids better if we exclude that powerful radiant on the edge of radiant display. On December 5 and 10 the ORN source is more active than ORS. In our last drawing for December 15 the ORS are only seen as a very weak source, and the ORN are probably hidden in the powerful Geminid radiant. But at the moment, conclusions about the χ-Orionid activity in December are not very trustworthy because of insufficient data.

Table 7 – Data for Figure 8 — the December radiant plots. N is the number of all meteors from that interval, n is the number of meteors actually contributing to the radiant plot.

Date	$\lambda_\odot$ [°]	v_∞ [km/s]	N	n
Dec 05	253.15	27	823	92
Dec 10	258.23	26	3215	671
Dec 15	263.31	29	4247	300

6.5 The radiant drift on the basis of 5°-solar longitude intervals

In Figure 6 (page 52) we can see the 5°-solar-longitude radiant drift of the Taurids. The same data are presented in Table 8; see also Figure 7. We can see on the graph showing the declination that the drift is not lin-

Table 8 – Positions for radiants of the Taurid complex calculated for 5°-solar-longitude intervals. The positions were measured on just one radiant display with the function 'Find'. The coordinates and the radius (R) of the biggest prominence of the radiant are given. The dates marked with '*' indicate the dates on which the positions of radiants are not certain, as they varied greatly between different velocity calculations.

Date	$\lambda_\odot$	NTA			STA			NPI			SPI			ORN		
		α	δ	R	α	δ	R	α	δ	R	α	δ	R	α	δ	R
5.9.	162.74	358	5	3	353	-7	2	354	3	2						
10.9.	167.59	4	5	3	10	-2	2	358	5	1	357	5	2			
15.9.	172.33	8	8	5	11	1	2	358	2	2						
20.9.	177.33	14	6	4	16	4	6	9	13	3	13	1	3			
25.9.	182.22	19	9	1	22	3	3	13	8	5	16	3	3			
30.9.	187.13	20	11	1	26	8	8	13	11	2						
5.10.	192.06				28	7	3	22	15	4						
10.10.	196.99	32	14	2	32	9	3	29	12	6						
15.10.	201.94	36	15	3	37	10	5									
20.10.	206.90	37	17	2	40	12	4									
25.10.	211.88	43	19	4	44	12	3									
30.10.	216.87	46	18	5	48	14	3									
5.11.	222.88	53	21	3	53	15	2									
10.11.	227.89	56	22	1	57	16	2									
15.11.	232.92	61	23	2	60	16	3							48	25	2
20.11.	237.97	66	24	2	65	16	2					ORS		57	23	1
25.11.	243.02	69	24	2	73	20	4							65	27	2
30.11.	248.08	76	22	3							76	14	3	72	24	1
5.12.*	253.15										82	19	2	78	25	2
10.12.*	258.23										89	20	3	85	27	3

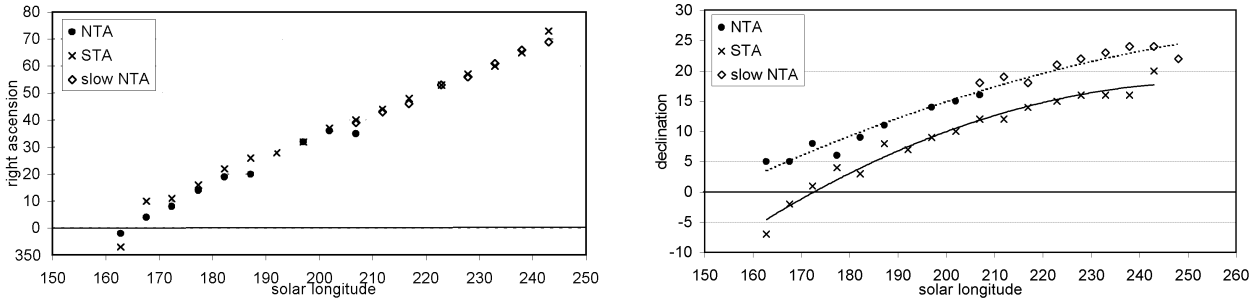

Figure 6 – Left: the progression of right ascension (α) and right: the progression of declination (δ) for 5-solar-longitude intervals of NTA (dots and diamonds) and STA (crosses). Until October 20 the NTA appear to be most prominent at lower velocities (dots) while they show up best for 30+ km/s in the second part of their activity period (open diamonds). The progression in declination is not linear, the best-fit function is quadratic here.

ear, as we expect from a radiant motion parallel to the ecliptic rather than the equator.

We can also see that the behavior of the separation from the actual line of the ecliptic is similar for both showers: in the beginning of their activity the separation it is big while at the end of activity it is small.

The best fitting quadratic functions through the 5°-solar-longitude Taurid declination radiant positions deliver:

$$\delta_{\mathrm{STA}} = -0.026\lambda_\odot^2 + 1.34\lambda_\odot - 153.08$$
$$\delta_{\mathrm{both\_NTA}} = -0.0013\lambda_\odot^2 + 0.76\lambda_\odot - 87.08\ .$$

The right ascensions can still be fitted with a linear function:

$$\alpha_{\mathrm{STA}} = 0.77\lambda_\odot - 120.27$$
$$\alpha_{\mathrm{both\_NTA}} = 0.86\lambda_\odot - 139.21\ .$$

The right ascension radiant drift obtained from 5°-solar-longitude intervals fits nicely with the radiant drift which we delivered out of 1°-solar-longitude intervals of just one month of Taurid activity.

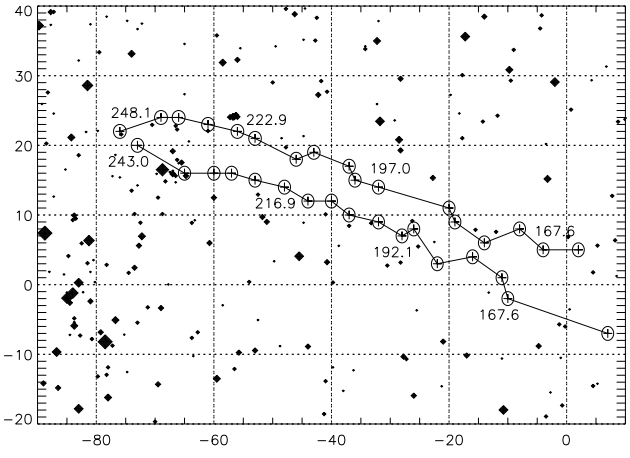

Figure 7 – Radiants of the Northern and Southern Taurids as derived from 5-day periods.

7 The beginning of Taurid activity and Piscids

As we saw in previous section, many aspects of the activity of the Taurid complex are unclear in September. Therefore we made another set of calculations — 2°-solar-longitude (≈ 2-day) periods ($(\lambda_\odot - 1) + 0.80 < \lambda_\odot < (\lambda_\odot + 1) + 0.80$). In Figure 1 we see that in September there are on average around 1000 meteors in 2-day intervals, which will be enough to check the detailed radiant drift. To get a broader view of different components of the Taurid complex activity, we now used a 0.°4 pixel size which gave an area of computation of $40° \times 40°$. As the Piscids are even less active than the Taurids we used meteors up to maximum distances of 70°; the plotting and velocity errors are from Table 2. We made a set of computations with different velocities (15, 18, 21, 26, 29, 33, 37, 40 km/s) for each interval.

7.1 The beginning of Taurid activity

Even on September 2 one prominent radiant is best seen at $v_\infty = 29$ km/s in the north part of the ecliptic at $\alpha = 357°$ and $\delta = 5°$. Can we say these are already Taurids? It is a twin radiant as seen in Figure 3 (September 5), with a weaker twin radiant further west parallel to the ecliptic. This weaker twin radiant could be a Northern Piscid radiant, as these can be active even from late August according to some catalogs (Cannon, 2001). We can easily follow this double radiant until September 10, when for one period the NPI almost disappear, though they are back on September 12. The third structure seen on the top of the NTA and NPI radiants in Figure 3 (September 5) at $\alpha = 358°$, $\delta = 8°$ can be followed through time just until September 8, and is best seen at velocities 26 and 29 km/s.

We also can follow an STA radiant from the beginning of September. It must be stated that at first it is a very weak source compared to NTA and even NPI radiants until September 10 and most prominent at $v_\infty = 26$ km/s. The STA's prominence overtakes that of the NTA on September 20, whereas an interval earlier they were the same. The STA are unambiguously seen only in the second part of September.

7.2 The Piscids

The NPI can be seen at velocities from 26 to 40 km/s. The NPI radiants are the most prominent somewhere at $v_\infty = 33$ km/s. They are less prominent than the NTA for the first part of September, but somewhere in the middle of that month they gain in prominence, unsurprisingly as the NTA reduce their activity. Their distance toward the ecliptic gets bigger until September 22, when on September 24 they jump back to the ecliptic.

Surprisingly, the SPI cannot be seen at the listed velocity of 29 km/s; maybe when we know where they stand from previous computations we can see a hint of them also at 26 km/s, but as already suggested they stand out at smaller v_∞ of 21 or even 18 km/s. At these velocities we can follow them easily for almost the whole of September, and they are the most prominent source.

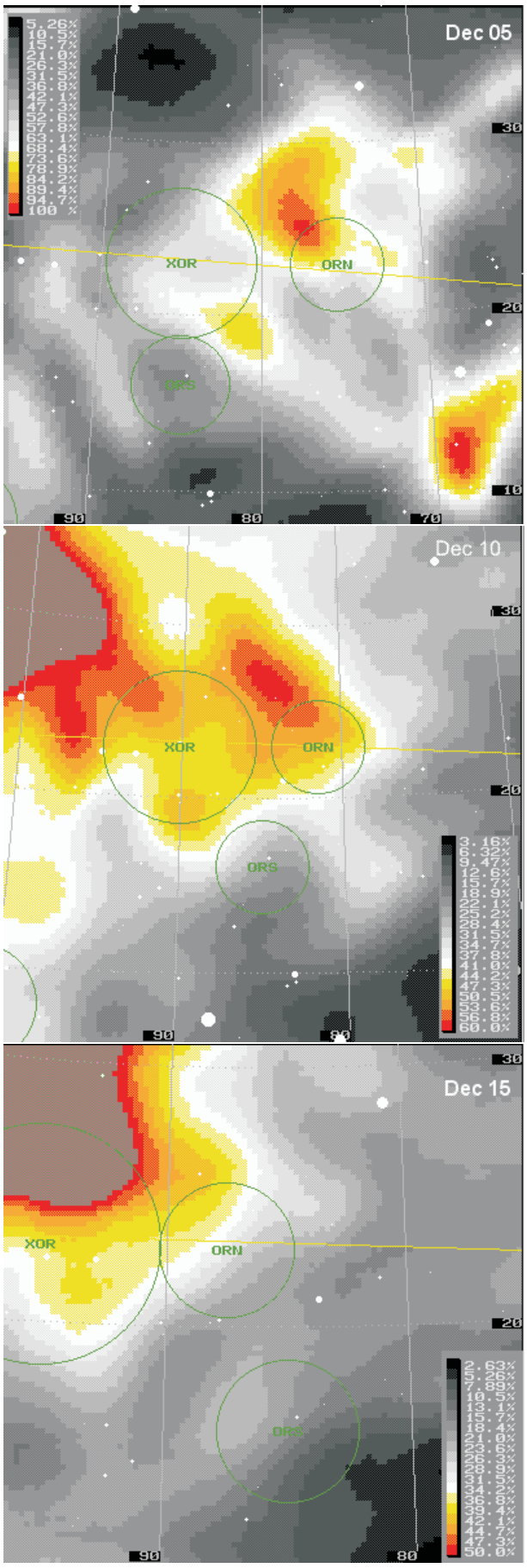

Figure 8 – December radiant plots. Prominence levels above 60% for December 10, and above 50% for December 15, are not displayed. For explanation see page 51.

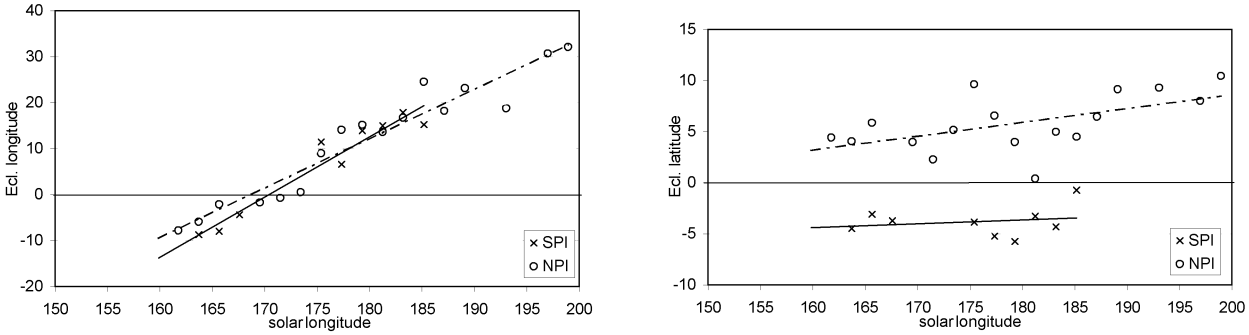

Figure 9 – Left: the progression of ecliptical longitude (l), right: the progression of ecliptical latitude (b) of the SPI and NPI.

7.3 The Piscid radiant drift derived from 2° solar longitude intervals

7.3.1 Southern Piscids

The radiant positions in Table 9 are computed as an average of radiant positions obtained for three velocities $v_\infty = 21$, 26 and 29 km/s. The error is a standard deviation, in this case just the bigger of the two standard deviations obtained for right ascension and declination. When comparing it with the errors obtained for the Taurid radiant drift, we now get much larger errors. This is because the SPI have even weaker activity than the Taurids and a few meteors make a big difference. The number of meteors used in calculations at different velocities n_{21} and n_{29} do not just include the SPI: there are also both branches of Taurids and also the NPI on the radiant drawing, so it must be stressed that the SPI meteors constitute a smaller fraction of this number.

At smaller velocities of $v_\infty = 18$ and 21 km/s we can see different radiant drawings with a bunch of radiants, but as we cannot follow those radiants in a set of more than two velocity classes we can conclude these are spurious radiants.

The SPI radiant can be followed as a relatively well-seen small prominence radiant in the interval from September 18 to September 28. This fits very well with the maximum of SPI activity on September 20 mentioned in (Rendtel et al., 1995) or the maximum interval September 18–21 mentioned by Dubietis (2001). One separate case of its appearance is September 6, when we can also see them as a separate radiant. On September 8 and 10 they are very weak, hopefully not just identified from a few meteors.

The regression through the points from $\lambda_\odot = 158\overset{\circ}{.}8$ to $\lambda_\odot = 188\overset{\circ}{.}8$ leads to an ecliptical coordinate drift of the SPI:

$$l = 337\overset{\circ}{.}36 + \lambda_\odot \cdot 1.31,\ b = -10\overset{\circ}{.}73 + \lambda_\odot \cdot 0.0394\ .$$

For the interval from September 1 to October 1 one day is 0.98° of solar longitude on average, from which the radiant drift is $0.98 \times 1.31 \simeq 1.28°$ per day.

The corresponding regression lines through the equatorial coordinates deliver for the SPI:

$$\alpha = 160.84° + \lambda_\odot \cdot 1.18°,\ \delta = -92.11° + \lambda_\odot \cdot 0.52°\ .$$

These equatorial coordinate results do not coincide with the SPI radiant drifts mentioned in (Rendtel et al., 1995), where $\Delta\alpha = 0.8°$ and $\Delta\delta = 0.2°$.

As the measured radiant positions have a void in them, it would be necessary to check the SPI radiant drift in a couple of years time, when more video data will have been gathered. It would also be recommended to get more meteors from the southern part of the sky as in September and October more than 2/3 of meteors are from the north side of ecliptic, and that probably causes such a low activity of the SPI.

7.3.2 Northern Piscids

The radiant positions in Table 10 are computed as an average of radiant positions obtained for three velocities: 26, 29 and 33 km/s. The error given in the table is the bigger of the right ascension and declination standard deviations. The NPI radiant becomes very weak in the interval September 26 to 28, but can be followed in all three velocity calculations. On September 30 the radiant can be seen as a separate very weak radiant only at $v_\infty = 26$ km/s, maybe hinted at also at 29 km/s. On October 6 it can be distinguished from the NTA only at higher velocities, when the outgrowth seen on Figure 4 (October 5) disintegrates into two parts, the upper of which is the NPI. On October 8 the NPI radiant is again the outgrowth from the NTA radiant, but we will not use it in the calculations of the regression line as the data sample is too small (133/481). In the last two intervals the NPI radiant is a weak outgrowth out of the NTA radiant, and again it can be seen as a separate radiant just at higher velocities of 33 and 37 km/s. On October 14 there is no sign of any separate NPI radiant even at higher velocities, and we can say they melt into the NTA radiant.

Again we can see the NPI radiant on October 16; it is seen only at higher velocities ($v_\infty = 33$, 37 and 40 km/s) at $\alpha = 28°$ and $\delta = 13°$. An interval further on October 18 the NPI present only a weak outgrowth from the NTA radiant, seen just at higher velocities, and we will not use it for the calculations as it is really weak.

We can say the NPI are detectable from September 4 to October 16: this is a very long interval of activity, already comparable with the Taurids. Their activity is all the time much weaker than that of the Taurids, and even that is very poor at this time of the year. We can say that the maxima of activity deduced only from the prominence of radiant plots are around September 20,

Table 9 – The radiant positions of the SPI (seen at $v_\infty = 21$, 26 and 29 km/s) calculated for 2° solar longitude intervals.

Date	$\lambda_\odot$	N	n_{21}	n_{29}	SPI				
					α	δ	err	l	b
2.9.	159.83	824	122	115					
4.9.	161.77	1543	244	244					
6.9.	163.71	936	154	151	354.0	-7.5	0.7	351.3	-4.5
8.9.	165.65	1169	198	194	354.0	-6.0	1.0	352.0	-3.1
10.9.	167.59	1135	199	194	357.5	-5.0	0.7	355.6	-3.7
12.9.	169.53	1063	128	168					
14.9.	171.48	982	163	165					
16.9.	173.43	933	162	164					
18.9.	175.38	927	163	161	12.0	1.0	0.5	11.4	-3.9
20.9.	177.33	874	158	160	8.0	-2.0	0.5	6.6	-5.2
22.9.	179.29	704	153	152	15.0	0.0	0.5	13.9	-5.8
24.9.	181.24	1076	190	188	15.0	3.0	0.5	15.0	-3.3
26.9.	183.21	889	189	190	18.0	3.0	0.5	17.8	-4.3
28.9.	185.17	516	107	115	14.5	3.5	0.7	15.2	-0.7
30.9.	187.13	1412	273	194					

Table 10 – The radiant positions of the NPI (seen at $v_\infty = 26$ to 40 km/s) and a unknown radiant in the beginning of September (seen at 26 to 33 km/s). The radiant positions for the dates marked with * were not included in calculations.

Date	$\lambda_\odot$	N	$n_{\min}$	NPI					unknown				
				α	δ	err	l	b	α	δ	err	l	b
2.9.	159.83	824	114										
4.9.	161.77	1543	231	351.0	1.0	0.0	352.2	4.4	352.0	7.0	1.0	355.7	9.7
6.9.	163.71	936	150	353.0	1.3	2.1	354.1	4.0	358.0	10.5	2.1	2.6	10.2
8.9.	165.65	1169	190	355.7	4.7	2.1	357.8	5.9	3.3	8.3	0.6	6.5	6.3
10.9.	167.59	1135	190										
12.9.	169.53	1063	167	356.7	3.0	1.5	358.3	4.0					
14.9.	171.48	982	159	358.3	1.7	0.6	359.3	2.3					
16.9.	173.43	933	162	358.3	5.0	2.6	0.5	5.2					
18.9.	175.38	927	157	4.3	12.3	2.3	9.0	9.6					
20.9.	177.33	874	156	10.3	11.7	0.6	14.1	6.6					
22.9.	179.29	704	146	12.5	9.5	0.7	15.1	4.0					
24.9.	181.24	1076	182	12.3	5.7	0.6	13.6	0.4					
26.9.	183.21	889	189	13.3	11.3	0.6	16.7	5.0					
28.9.	185.17	516	107	21.0	13.7	2.6	24.6	4.5					
30.9.	187.13	1412	268	14.0	13.0	0.5	18.2	6.5					
2.10.	189.10	845	193	18.7	15.7	0.6	23.1	9.1					
4.10.	191.07	657	142										
6.10.	193.04	437	109	13.7	16.0	1.0	18.8	9.3					
8.10.*	195.01	481	133										
10.10.	196.99	900	198	25.7	19.0	1.0	30.7	8.0					
12.10.	198.97	1677	347	26.0	22.0	1.4	32.1	10.5					
14.10.	200.95	1324	284										
16.10.*	202.93	2811	499	28.0	13.0	1.0	30.5	1.6					
18.10.*	204.90	1934	353	26.0	22.0	3.0	32.1	10.5					

September 24 and October 2; at those three 2°-solar-longitude intervals the prominence of the NPI radiants becomes comparable with the most active branch of the Taurids at that time. The variability is not considered physical, though. We have to admit that the Piscid radiants are much more difficult to follow than the Taurid radiants.

The regression through the points from $\lambda_\odot = 158\overset{\circ}{.}8$ to $\lambda_\odot = 200\overset{\circ}{.}8$ leads to an ecliptical coordinate drift of the NPI as given below. Again no reference $\lambda_\odot$ is given as no exact maximum can be found in different sources (Rendtel et al., 1995).

$$l = 178.4^\circ + \lambda_\odot \cdot 1.08,\ b = -18.6^\circ + \lambda_\odot \cdot 0.1362$$

Corresponding regression lines through the equatorial coordinates deliver for the NPI:

$$\alpha = 197.14^\circ + \lambda_\odot \cdot 0.95,\ \delta = -86.08^\circ + \lambda_\odot \cdot 0.53$$

8 Conclusions

When comparing the radiant plots obtained for the Taurid radiants and the Perseid radiant (Arlt, 2003) at the same scale of radiant display, it is obvious that the Taurid radiants are larger than the Perseid radiant. Both were derived from video observations and for the same calculation parameters.

The Taurid meteor shower complex as a clear double source is active from mid-September to November 25. The Northern Taurids exhibit strongest radiation areas for relatively large pre-atmospheric velocities up to about October 20. We estimate the velocity to be 33 km/s on average. During the second part of activity, a lower entry velocity seems appropriate such as v_∞ = 26 km/s which is actually the value listed in the IMO Working List of visual meteor showers. At the transition between the two periods, the match with Babadzhanov's (2001) NTA having their maximum on October 24 and $v_\infty = 29.7$ seems good.

The Southern Taurids are active from the beginning of September to November 20, while until September 10 their activity is very low, as the weaker SPI outnumber them. The STA cannot be divided into separate branches and do not show a migration through a velocity range as was suggested for the NTA.

The radiant drift in ecliptical coordinates for the October–November period, derived in 1°-longitude intervals, is

$$\Delta l_{\mathrm{NTA}} = 0.83^\circ, \qquad \Delta l_{\mathrm{STA}} = 0.78^\circ.$$

The radiant drift of both branches in right ascension is

$$\Delta\alpha_{\mathrm{STA}} = 0.77^\circ,$$
$$\Delta\alpha_{\mathrm{both\_NTA}} = 0.86^\circ.$$

The radiant drift of declination is not linear:

$$\delta_{\mathrm{STA}} = -0.026\lambda_\odot^2 + 1.34\lambda_\odot - 153.08,$$
$$\delta_{\mathrm{both\_NTA}} = -0.0013\lambda_\odot^2 + 0.76\lambda_\odot - 87.08.$$

We used linear fits through the ecliptical coordinates to construct a smooth radiant drift for the period September 10 to November 30 and suggest this motion for future issues of the IMO Working List of visual meteor showers (see Table 11 and Figure 10). The dates refer to 00^{h} UT, and we have chosen the year 2009 for the solar-longitude-to-date conversion because this is a very 'average' year in terms of leap-year wobble.

Table 11 – Proposed radiant drift table for the Northern and Southern Taurids.

Date	α_{NTA}	δ_{NTA}	α_{STA}	δ_{STA}
Sep 10	7.3	+6.0	10.2	+2.1
Sep 15	11.1	+7.6	13.8	+3.4
Sep 20	14.9	+9.1	17.4	+4.7
Sep 25	18.7	+10.6	21.0	+5.9
Sep 30	22.5	+12.1	24.6	+7.1
Oct 05	26.4	+13.6	28.3	+8.3
Oct 10	30.4	+15.0	32.0	+9.5
Oct 15	34.4	+16.4	35.8	+10.6
Oct 20	38.5	+17.7	39.6	+11.6
Oct 25	42.7	+18.9	43.4	+12.6
Oct 30	46.9	+20.0	47.3	+13.5
Nov 05	52.0	+21.3	52.0	+14.5
Nov 10	56.4	+22.2	56.0	+15.2
Nov 15	60.8	+23.1	60.0	+15.8
Nov 20	65.3	+23.8	64.1	+16.4
Nov 25	69.8	+24.4	68.1	+16.8
Nov 30	74.4	+24.9	72.2	+17.2

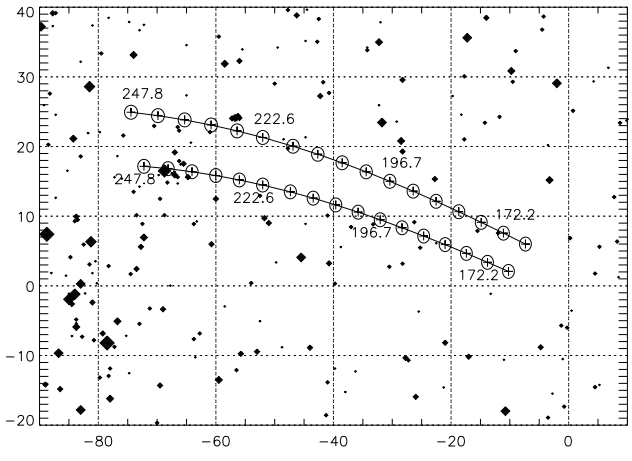

Figure 10 – Suggested average radiant drifts of the Northern and Southern Taurids.

With respect to the Piscids, we find that the most prominent source is the NPI radiant, although it is a much weaker source than the Taurids in September. The NPI are detectable from September 4 to October 18. Based on the constant visibility of the NPI radiant for the velocities 21, 26, 29 km/s, we conclude that the most probable velocity of NPI is v_∞ =26 km/s. The SPI are hardly detectable: we can follow them in the intervals September 6–10 and September 18–28 (seen in 2° solar longitude intervals), with the latter exhibiting the more prominent SPI. Based on the constant visibility of SPI for velocities 26, 29, 33 km/s, we conclude that the most probable velocity of the SPI is v_∞ =30 km/s. The radiant drift in ecliptical coordinates derived from the 2° solar longitude intervals is $\Delta l_{\mathrm{SPI}} = 1.31^\circ$ and $\Delta l_{\mathrm{NPI}} = 1.08^\circ$. The radiant drift in

equatorial coordinates is $\Delta\alpha_{\mathrm{SPI}} = 1.18°$, $\Delta\delta_{\mathrm{SPI}} = 0.52°$ and $\Delta\alpha_{\mathrm{NPI}} = 0.95°$, $\Delta\delta_{\mathrm{NPI}} = 0.53°$.

The χ-Orionids appear to exhibit two separate branches in the 5° solar longitude interval calculations. The northern branch appears first on November 15, the southern branch on November 30. There are too few data to derive any detailed radiant drift of either branch.

Acknowledgments

This paper would have been impossible without the tremendous work of Sirko Molau in setting up and maintaining the IMO video network. We are very grateful for his efforts and also for providing the databases. We would also like to thank the video observers whose data contributed to this analysis.

References

Asher, D.J. (1994), "The Taurid meteor complex", New College, Oxford, PhD thesis.

Asher, D.J., Steel, D.I. (1995), "Theoretical meteor radiants for macroscopic Taurid Complex objects", *Earth, Moon and Planets* **68**, 155–164.

Arlt, R. (1992), "The software Radiant", *WGN* **20**, 62–69.

Arlt, R. (2000), "Glancing at the Taurids of the last decade", *IMC Proceedings 1999* 112-120.

Arlt, R. (2001), "The Radiant software – details and problems scrutinized", *IMC Proceedings 2000* 10–17.

Arlt, R. (2003), "Radiant ephemeris for the Perseid meteor shower", *WGN* **31:1**, 19–28.

Babadzhanov, P.B. (2001), "Search for meteor showers associated with Near-Earth Asteroids: I. Taurid Complex", *Astronomy and Astrophysics* **373**, 329–335.

Bellot Rubio, L.R. (1994), "An analysis of the Taurid radiants", *WGN* **22**, 108–110.

Cannon, E. (2001), "Visual Meteor Showers/Meteor Streams in order of Date of Maximum (a compilation from different sources)", `http://web.austin.utexas.edu/edcannon/aka-date.htm`

Denning, W.F. (1883), "The Taurids", *The observatory* **6**, 154.

Denning, W.F. (1901), "The November Taurids", *The observatory* **24**, 52–54.

Dubietis, A. (2001), "Activity of the Southern Piscid Meteor Shower in 1985-1999", *WGN* **29:1/2**, 29–35.

Jenniskens, P. (1997), "Meteor stream activity I. The annual streams", *Astronomy & Astrophysics* **287**, 990–1013.

Klačka, J. (1995), "The Taurid complex of asteroids", *Astronomy & Astrophysics* **295**, 420–422.

McBeath, A. (1999), "On the occurrence of bright Taurids", *WGN* **27:1**, 53–56.

Molau, S. (1999), "The meteor detection software MetRec", *IMC Proceedings 1998* 9–16.

Molau, S. (2005a), "IMO video network database", `http://www.metrec.org/database.html`

Molau, S. (2005b), "personal communication".

Porubčan, V., Kornoš, L. (2002), "The Taurid meteor shower", *Proceedings of Asteroids, Comets, Meteors – ACM 2002 (Berlin)* 177–180.

Rendtel, J., Arlt, R., McBeath, A. (1995), "Handbook for visual meteor observers", *IMO*.

Shigeno, Y., Shioi, H. (2002), "Outburst of Faint Piscids in 2001", *WGN* **30:3**, 56–58.

Steel, D.I., Asher, D.J., Clube, S.V.M. (1991), "The structure and the evolution of the Taurid complex", *Mon. Not. Roy. Astr. Soc.* **251**, 632–648.

Triglav, M. (1999), "The analysis of two Taurid radiants from plotted meteors", *IMC Proceedings 1998* 75–81.

Triglav, M. (2000), "The analysis of two Taurid radiants from 10 years of plotted meteors", *IMC Proceedings 1999* 101–11.

Table 12 – The Taurid radiant positions calculated for 1° solar longitude intervals. The pre-atmospheric velocities assumed for the computations are 27 km/s for NTA and 29 km/s for STA.

Date	$\lambda_\odot$	N	$n_{\min}$	NTA					STA				
				α	δ	err	l	b	α	δ	err	l	b
3.10.	190.06	318	63						25.55	5.36	0.2	25.64	-4.88
4.10.*	191.04	303	27										
5.10.	192.02	244	54						28.02	8.25	0.3	29.00	-3.07
6.10.	193.00	394	79						29.93	8.38	0.2	30.85	-3.55
7.10.	194.00	237	63						28.69	9.47	0.1	29.97	-2.15
8.10.	195.00	328	79						29.37	8.29	0.3	30.21	-3.52
9.10.*	195.96	179	45										
10.10.	196.96	342	90						32.01	8.76	0.2	32.89	-3.96
11.10.	197.96	449	85						34.48	10.35	0.2	35.67	-3.24
12.10.	198.94	517	114						32.94	11.37	0.2	34.58	-1.80
13.10.	199.94	769	152	33.58	15.54	0.8	36.53	1.96	34.93	10.77	0.8	36.27	-3.03
14.10.	200.92	806	130						35.34	10.74	0.2	36.65	-3.16
15.10.	201.92	785	164						36.76	10.22	0.2	37.78	-4.07
16.10.	202.92	979	162						37.22	10.53	0.5	38.35	-3.95
17.10.	203.90	1577	239	37.66	17.63	0.2	40.93	2.67	38.19	9.81	0.3	38.98	-4.90
18.10.	204.89	1134	197						38.47	11.38	0.1	39.72	-3.55
19.10.	205.89	942	162	39.53	16.39	0.4	42.25	0.88	39.79	13.36	0.4	41.53	-2.04
20.10.	206.86	777	152	39.40	17.81	0.3	42.61	2.33	39.85	12.11	0.2	41.26	-3.21
21.10.	207.86	466	67	37.40	16.85	0.2	40.50	1.96	41.15	12.26	0.3	42.53	-3.51
22.10.*	208.86	336	45										
23.10.	209.86	967	153	40.56	20.44	0.3	44.34	4.50	42.96	12.64	0.2	44.33	-3.65
24.10.	210.86	1018	140	40.90	17.18	0.2	43.75	1.24	43.48	11.99	0.1	44.60	-4.46
25.10.	211.86	740	128	41.93	19.28	0.6	45.32	2.95	43.37	11.36	0.2	44.32	-5.00
26.10.	212.86	410	92	44.28	22.86	0.4	48.45	5.75	45.61	12.32	0.2	46.78	-4.69
27.10.	213.86	824	146	46.25	19.32	0.4	49.27	1.86	45.78	12.95	0.2	47.05	-4.15
28.10.	214.86	745	132	46.84	18.84	0.3	49.60	1.24	46.29	13.41	0.4	47.58	-3.78
29.10.**	215.86	444	79						49.61	13.81	0.2	50.89	-4.29
30.10.	216.86	176	50	46.90	20.11	0.1	50.07	2.46	48.98	14.01	0.2	50.37	-3.94
31.10.**	217.86	209	52						48.62	14.50	0.3	50.12	-3.35
1.11.	218.86	265	61	45.83	20.89	0.2	49.31	3.41	48.23	15.32	0.5	49.95	-2.47
2.11.**	219.86	376	65						47.90	14.75	0.1	49.50	-2.97
3.11.	220.86	760	177	50.62	20.63	0.1	53.52	2.06	51.35	14.35	0.5	52.69	-4.23
4.11.	221.88	455	126	52.21	19.51	0.2	54.69	0.61	51.66	14.62	0.2	53.05	-4.02
5.11.	222.88	446	96	52.90	20.66	0.2	55.64	1.49	54.29	13.92	0.3	55.30	-5.28
6.11.	223.88	575	113	53.68	21.72	0.2	56.64	2.41	54.17	14.14	0.2	55.25	-5.06
7.11.	224.88	469	110	54.66	21.31	0.2	57.42	1.81	54.39	15.13	0.2	55.68	-4.14
8.11.*	225.88	140	27										
9.11.*	226.88	248	45										
10.11.	227.88	243	77	56.38	21.61	0.1	59.04	1.73	56.32	15.82	0.1	57.69	-3.90
11.11.	228.88	427	106	56.69	22.65	0.1	59.46	2.65					
12.11.	229.90	301	76	57.39	22.03	0.3	59.98	1.92	55.71	15.58	0.2	57.06	-4.05
13.11.	230.91	152	50	59.26	22.77	0.4	61.88	2.25	56.93	16.37	0.2	58.32	-3.52
14.11.	231.91	346	88	59.09	22.84	0.2	61.71	2.39	58.92	15.43	0.1	60.07	-4.84
15.11.	232.92	378	62	61.22	23.18	0.2	63.72	2.28	58.56	13.42	0.1	59.34	-6.72
16.11.	233.92	747	129	60.95	24.18	0.2	63.67	3.31	62.75	16.52	0.2	63.89	-4.47
17.11.	234.92	1285	229	64.33	23.19	0.4	66.54	1.77	61.27	15.78	0.2	63.24	-5.15
18.11.	235.92	1121	215	63.80	24.21	0.1	66.25	2.94	63.69	16.07	0.3	63.69	-4.94
19.11.	236.92	2283	257	63.80	24.69	0.1	66.32	3.33	63.07	15.85	0.3	64.04	-5.21
20.11.	237.95	636	137	67.94	23.27	0.3	69.79	1.34	63.04	15.62	0.3	64.00	-5.41
21.11.*	238.97	109	21										
22.11.	239.97	372	96	67.70	23.69	0.3	69.66	1.77					

Electrophonic meteors

VLF monitoring of the Genesis Sample Return Capsule re-entry

Martin Beech[1,2] *and Ian Murray*[2,3]

We report on an experiment to monitor the very low frequency (VLF) electromagnetic radiation background emission during the time of the Genesis sample return capsule (SRC) re-entry on 2004 September 8. No distinctive re-entry related VLF signal was detected. With respect to the magnetic entanglement model for electrophonic sound generation, we find that the Reynolds number in the ablation flow must apparently exceed 3–5×10^5 before VLF electromagnetic radiation generation can proceed.

Received 2005 February 24

1 Introduction

The entry of meter-sized bodies, at hypersonic speeds, into the Earth's atmosphere produces a number of distinct visual and acoustic phenomena. Amongst the acoustic phenomena is the generation of electrophonic (or simultaneous) sounds (Keay, 1980, 1992, 1993). Numerous bright fireballs throughout recorded history have been reported to produce simultaneous sounds, and in the case of meteorite dropping events they are often accompanied by a second acoustic phenomenon in the form of time delayed sonic booms. Sustained electrophonic sounds, it has been argued, are produced by the entanglement of the geomagnetic field within the plasma column behind the ablating meteoroid. Keay's pioneering explanation of electrophonic sounds is based upon the generation of VLF electromagnetic radiation by the relaxing geomagnetic field. Audible sounds are then produced through the transduction of the VLF radiation by objects situated close to the observer (Keay and Ostwald, 1991).

The inherent problem in attempting to experimentally verify the first stage of the electrophonic sound production mechanism, namely the generation of VLF electromagnetic radiation, is the mainly unpredictable time of fireball appearances. This situation was partially addressed during the recent spate of Leonid meteor storms, when the probability of recording fireball events was greatly enhanced over normal. Zgrablić et al., (2002), for example, have reported on the apparent instrumental detection of electrophonic sounds during the 1998 Leonids, but their study found no clear correspondence between the generation of the sounds recorded and the production of a distinct VLF signal. Price and Blum (1998), on the other hand, report on the detection of distinct VLF radiation signatures from Leonid meteors, but their experiment could not verify the generation of actual electrophonic sounds. Likewise, (Beech et al., 1995) have reported on the detection of a distinct VLF radiation signal, from a detonating fireball observed on 1993 August 11, but this event did not generate any reported electrophonic sounds.

Electrophonic sounds have been reported to accompany the destruction of re-entering spacecraft. In Canada, for example, the 1978 January 24th re-entry of the Cosmos 954 satellite was accompanied by multiple accounts of electrophonic sounds (Heaps, 1978; Beech, 2004). Also, the re-entry of the Molynia 1–67 satellite over Western Australia on 2000 January 27 produced one reported case of electrophonic sound detection (Verveer et al., 2000). This latter re-entry event also produced a distinct magnetic disturbance recorded at several monitoring stations — indicating a clear interaction between the re-entering spacecraft and the Earth's magnetic field.

2 The Genesis mission

The launch of the Genesis sample return mission took place in August of 2001. Once inserted into its designated halo orbit at the first Lagrange point of the Earth–Sun system, the spacecraft sampled solar wind particles for some 850 days. In April of 2004 the spacecraft was brought back from interplanetary space to the Earth's orbit and the collecting arrays, housed in a protective SRC, were detached from the main spacecraft bus and maneuvered into a re-entry trajectory. Re-entry commenced on 2004 September 8th at $15^h52^m57^s$ UT, bringing the SRC to ground in Northwestern Utah.

The initial re-entry speed of the SRC was some 10.8 km/s, one of the highest ever re-entry speeds for a returning space capsule. The SRC dimensions were some 1.5 m in diameter by 0.5 m in length. These speed and size characteristics combine to make the Genesis SRC an ideal object to study with respect to the entry of meter-sized objects at hypersonic speeds into the Earth's upper atmosphere. Indeed, the re-entry speed, size and heating characteristics of the SRC were a close analog to those expected of a meteorite-dropping fireball event. Numerous video and spectroscopic experiments were positioned, by various research groups, to monitor the SRC re-entry (see, for example, the HYPERSSED MAC mission web page at `reentry.arc.nasa.gov/index.html`.)

3 Observations

The approximate ground path of the re-entering Genesis SRC is shown in Figure 1. The planned SRC capture was scheduled to take place over the US Air Force's

[1]Campion College, the University of Regina, Regina, SK, Canada S4S 0A2. Email: `beechm@uregina.ca`
[2]Department of Physics, the University of Regina, Regina, SK, Canada S4S 0A2
[3]Email: `ismrry@yahoo.ca`

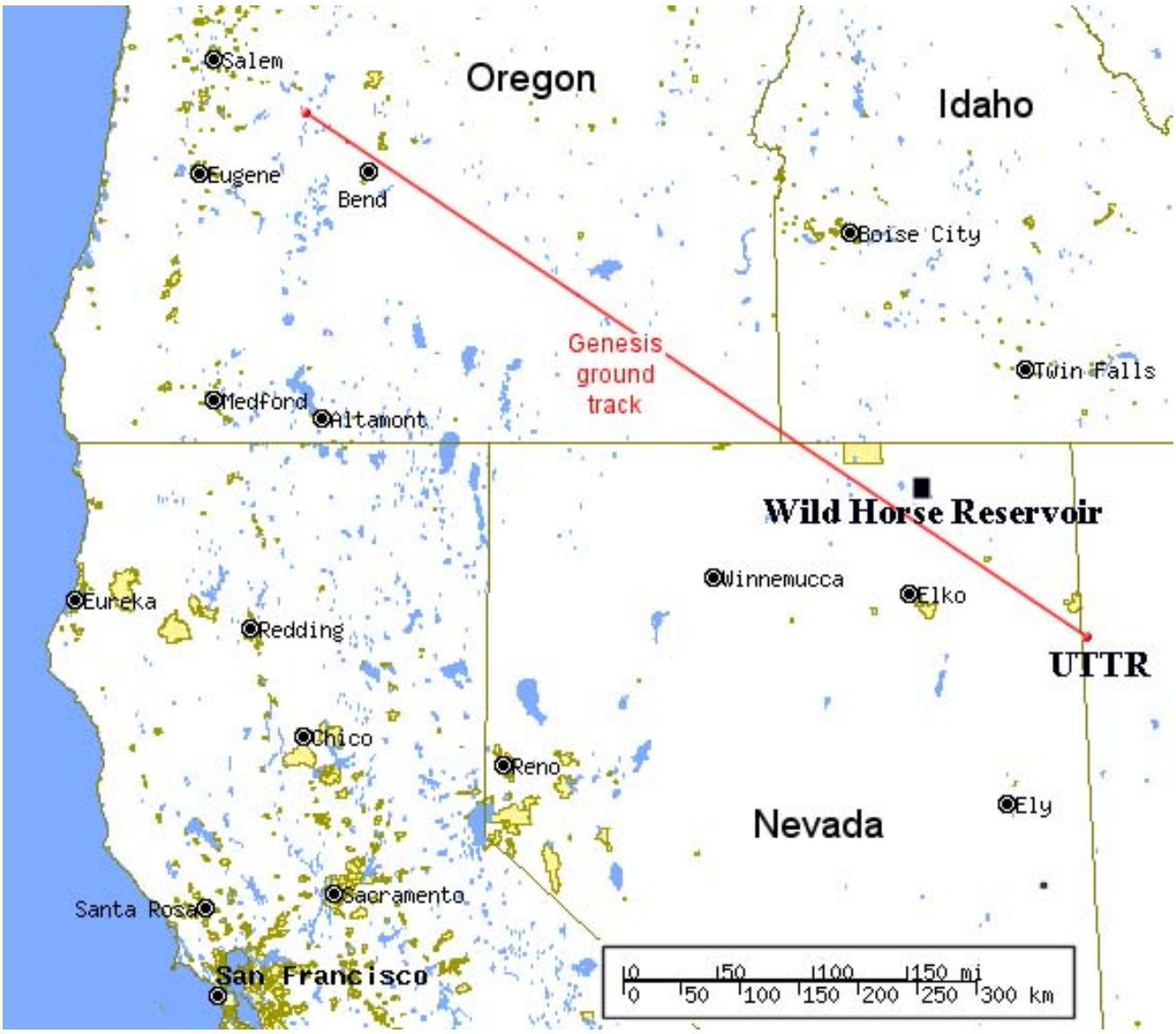

Figure 1 – The ground track of the re-entering Genesis SRC. The black square some 80 km north of Elko, Nevada indicates the approximate location of Wild Horse Reservoir.

Utah Test and Training Range (UTTR) in Northwestern Utah, but maximum heating was predicted to occur while the SRC was situated over Northeastern Nevada. Our experiment was accordingly located at Wild Horse Reservoir (some 80 km north of Elko, Nevada). Our observing location (latitude 41°40′2 N; longitude 115°48′1 W) was situated some 25 km from the ground track (at closest approach), and at an estimated range of 70 km from the SRC at the time of maximum heating. The experiment consisted of two VLF receivers with wire wound loop antennas. The VLF receivers are sensitive to frequencies between 1 and 30 kHz. The square antenna frames have 1 m sides and each antenna is wound from a 250 m length of insulated wire of 28 s.w.g. (standard wire gauge). The VLF receiver output and visual data were recorded onto Sony 120, Hi8 videotape. One antenna was orientated in a north-south direction while the other was placed in an east-west orientation. Testing of the receivers indicated that the location was interference-free and the various 'clicks', 'chirps' and 'whistlers' from the natural VLF background could be clearly heard. Figure 2 shows the experiment as it was deployed at Wild Horse Reservoir.

On the morning of September 8th we recorded the VLF background signal from both systems continuously over the time interval from $15^{h}45^{m}00^{s}$ to $16^{h}15^{m}00^{s}$ UT. This time interval covered the SRC re-entry window. We made no visual sighting of the SRC, but a distinct sonic boom was heard from our observing location at $15^{h}57^{m}12^{s}$ UT. Observers situated some 70 km to the east of our location did make a visual sighting of the SRC for about 15 seconds starting at $15^{h}53^{m}44^{s}$ UT, and the peak visual brightness was estimated to have been of order magnitude −9 (D. Hladiuk, personal communication). A second research group also located at Wild Horse Reservoir did detect a forward scatter radio transmission from the SRC re-entry ionization trail (R. Suggs, NASA Marshal Space Flight Center, personal communication). No distinct VLF signal, which could be related to the SRC re-entry, was recorded in either of our systems. Natural VLF background 'sounds' were audible throughout the entire recording interval.

Figure 2 – 'Camp Campion' at Wild Horse Reservoir, Nevada. The two antennas and tripods for the video cameras can be seen in photograph. The remote location of the campground ensured that the VLF reception was free from domestic electronic and electric power line interference.

4 Discussion

Keay (1980, 1992, 1995) has argued that VLF generation will proceed once the actual atmospheric height of a meteoroid (or spacecraft) falls below the transition altitude at which the flow in its associated ablation column becomes turbulent. The transition to turbulence is typically taken to be the attainment of a Reynolds number in excess of 10^6. The Reynolds number (Re) is expressed in terms of the velocity (V), the atmospheric density (ρ), the dynamic viscosity (μ_0) and the characteristic size of the body (L), such that $\mathrm{Re} = V\rho L/\mu_0$. In this analysis the characteristic dimension L is taken to be 1.5 m, the diameter of the Genesis SRC, and the velocity and atmospheric density as a function of atmospheric height are derived from the best fit SRC re-entry trajectory (P. Desai, personal communication). Table 1 is a summary of variation of the Reynolds number as a function of SRC altitude and velocity during re-entry. The density is taken from an MSIS-E-90 model atmosphere[1] applicable to the time, date and location of the observations. The maximum SRC heating is predicted to have occurred at an altitude of 60 km (Desai et al., 2000), and we can see from Table 1 that the flow would not have been turbulent at that altitude. The transition to turbulence, where the Reynolds number began to exceed 10^6, occurred at a height of some 25 km, well after the time of maximum heating. At the time of maximum heating the Reynolds number is estimated to have been of order $3–5\times10^5$.

The Genesis SRC re-entry was the first of several re-entry events that will be taking place during the next several years. The Stardust cometary dust-sampling mission is due to re-enter the Earth's atmosphere in January of 2006 while the Hayabusa (formerly MUSES–C) asteroid sample return mission is due to re-enter in June of 2007. The Stardust SRC is about half the size of the Genesis SRC, but will enter the atmosphere at a slightly higher initial speed of 12.9 km/s (Desai et al., 1997). The Hayabusa SRC is about one quarter of the size of the Genesis SRC, and will have an initial entry velocity of some 11.6 km/s. The smaller dimensions of the Stardust and Hayabusa SRCs dictate that the onset of turbulence conditions in their associated wakes will be at lower altitudes than those derived for the Genesis SRC. This condition in turn suggests that no distinct VLF electromagnetic radiation emission should be produced during the re-entry of either the Stardust SRC or the Hayabusa SRC. This result should hold true even though the initial velocities will be higher and the

[1]Documentation and software can be found at `http://nssdc.gsfc.nasa.gov/space/model/atmos/msise.html`

Table 1 – Height H, velocity V and Reynolds number Re for the Genesis SRC re-entry. The height and velocity data are from P. Desai (personal communication), and the Reynolds number calculation assumes a characteristic size of $L = 1.5$ m, and we assume a constant dynamic viscosity of $\mu_0 = 1.5 \times 10^{-5}$ Ns/m^2. The transition to turbulence occurred at an altitude of about 25 km. The SRC experienced its maximum heating at an estimated altitude of 60 km.

H (km)	V (m/s)	Re
70	1.05×10^4	8.44×10^4
65	1.01×10^4	1.70×10^5
60	9.46×10^3	2.97×10^5
55	8.22×10^3	4.86×10^5
50	6.42×10^3	7.08×10^5
45	3.85×10^3	8.06×10^5
40	1.84×10^3	7.71×10^5
35	816.7	7.22×10^5
30	400.0	7.70×10^5
25	259.6	1.09×10^6
20	232.7	2.18×10^6
15	149.2	3.13×10^6
10	100.0	4.17×10^6

peak heating rates greater than those experienced by the Genesis SRC (Desai et al., 2000).

5 Conclusions

We monitored emissions from the VLF electromagnetic radiation background during the time of the Genesis SRC re-entry on 2004 September 8th, but detected no distinctive re-entry related signal. At the time of maximum heating (altitude ∼60 km) the range of the SRC was some 70 km from our observing site. We estimate that at the time of maximum heating the Reynolds number in the ablative flow would have been below the turbulence limit of 10^6. The lack of any distinct re-entry related VLF signal is presumably due to the non-attainment of the turbulence condition at the time of peak heating. With respect to the magnetic entanglement model developed by Keay (1980, 1992, 1995), it would appear that a Reynolds number in excess of $3–5 \times 10^5$ is required in the ablation stream before the onset of VLF electromagnetic radiation generation can proceed.

Acknowledgments

The authors extend there thanks to Dr. Presun Desai (NASA Langley Research Center) for providing data relating to the SRC re-entry conditions. This research has been partially supported by a grant to MB from the Natural Sciences and Engineering Research Council of Canada.

References

Beech M. (2004). "The Millman Fireball Archive II: Sound reports". *J. Roy. Ast. Soc. Canada*, **98**, 34 – 41.

Beech M., Brown P., and Jones J. (1995). "VLF detection of fireballs". *Earth, Moon, Planets*, **68**, 181 – 188.

Desai P. N., Mitcheltree R. A., and Cheatwood F. M. (1997). "Entry dispersion analysis for the Stardust comet sample return capsule". In *Proc. American Institute of Aeronautics and Astronautics Conference, New Orleans, LA*, pages 1–11.

Desai P. N., Mitcheltree R. A., and Cheatwood F. M. (2000). "Sample returns missions in the coming decade". In *Proc. 51st International Astronautical Congress, Rio de Janeiro, Brazil*, pages 1–11.

Heaps L. (1978). *Operation Morning Light: terror in our skies, the true story of Cosmos 954*. Paddington Press, New York.

Keay C. S. L. (1980). "Anomalous sounds from the entry of meteor fireballs". *Science*, **210**, 11–15.

Keay C. S. L. (1992). "Electrophonic sounds from large meteor fireballs". *Meteoritics*, **27**, 144 – 148.

Keay C. S. L. (1993). "Progress in explaining the mysterious sounds produced by very large meteor fireballs". *J. Sci. Exploration*, **7:4**, 337 – 354.

Keay C. S. L. (1995). "In quest of meteor sounds". *Sky and Telescope*, **70**, 623–625.

Keay C. S. L. and Ostwald P. M. (1991). "A laboratory test of the production of electrophonic sounds". *J. Acoust. Soc. Am.*, **89:1**, 1823 – 1824.

Price C. and Blum M. (1998). "ELF/VLF radiation production by the 1999 Leonid meteors". *Earth, Moon, Planets*, **82/83**, 545 – 554.

Verveer P. A., Bland P. A., and Bevan A. W. R. (2000). "Electrophonic sounds from the reentry of the Molynia 1-67 satellite over Australia: confirmation of the electromagnetic link". *Meteoritics Plan. Sci. Suppl.*, **35:5**, A163–164.

Zgrablić G., Vinković D., Gradečak S., Kovačić D., Biliškov N., Grbac N., Andreić Ž., and Garaj S. (2002). "Instrumental recording of electrophonic sounds from Leonid fireballs". *J. Geophys. Res.*, **107:7A**, 10.1029–1132.

Ongoing meteor work

SPA Meteor Section results: an overview of the 2004 Ursids

Alastair McBeath [1]

An analysis of data collected by the SPA Meteor Section from the Ursids in 2004 is presented. The ZHRs found, although giving often poor coverage, were remarkably consistent on December 22, averaging $\sim 17 \pm 2$ between $\sim 03^{\rm h}$–$14^{\rm h}$ UT, but without giving a more clear-cut maximum. Radio data supported a more probable peak at some point between $\sim 09^{\rm h}$–$15^{\rm h}$ UT on December 22, most likely between $12^{\rm h}$–$14^{\rm h}$ UT.

Received 2005 January 29

1 Introduction

A late prediction by Esko Lyytinen and Markku Nissinen, issued on the IMO-News e-mailing list on 2004 December 21, suggested some very old meteoroid trails, laid down by Comet 8P/Tuttle in 801, 815, 829, 843, 856 and 1048 AD, might produce detectable enhancements in the 2004 Ursids. The suggested timings for these were all on December 22, at around $01^{\rm h}$–$02^{\rm h}$ UT for the 1048 trail, between roughly $10^{\rm h}$–$11^{\rm h}$ UT for the 843 and part of the 829 trails, and from approximately $11^{\rm h}30^{\rm m}$–$14^{\rm h}$ UT for the remaining ones plus another part of the 829 trail. The possible activity was unknown, but might be low to nonexistent — or hopefully higher. This was in addition to the normal maximum on the same date, due sometime between $07^{\rm h}$–$09^{\rm h}$ UT according to the 2004 IMO Meteor Shower Calendar.

Postings on IMO-News and the Meteorobs e-mail lists in the days following this announcement gave somewhat conflicting indications. As so often with the Ursids, the weather halted many observers' efforts — no UK visual results were received on them at all, for instance. Thanks to the kind help of Rich Taibi in the USA (who forwarded details from the American Meteor Society's results — see `www.amsmeteors.org`) and Chris Steyaert in Belgium (editor of the 'Radio Meteor Observations Bulletins', RMOBs; see `www.rmob.org`), plus all the observers listed below, I am able to offer this short analysis of the visual and radio data received.

Grateful thanks go to all the contributing observers, who included:

Visual – Robin Gray (Nevada, USA), Bob Lunsford (California, USA), Jürgen Rendtel (Germany; data posted on IMO-News on December 22), Wesley Stone (Oregon, USA) and Rich Taibi (Maryland, USA).

Radio – (data in 'RMOB 137', December 2004) Enric Fraile Algeciras (Spain), Jeff Brower (Colorado, USA), Alessandro & Giuseppe Candolini (Italy), Gaspard de Wilde (Belgium), David Entwistle (England), Ghent University (Belgium), Steve Hansen (Massachusetts, USA), Stan Nelson (New Mexico, USA), Sadao Okamoto (Japan), Mike Otte (Illinois, USA), Marcel Schneider (Luxembourg), Dave Swan (England), Istvan Tepliczky (Hungary) and Ilkka Yrjölä (Finland).

[1] 12a Prior's Walk, Morpeth, Northumberland, NE61 2RF, England, UK. Email: `meteor@popastro.com`

Analyses were carried out as normal, the ZHRs computed using the IMO's standard methods, assuming $r = 3.0$ for the Ursids. As some observers mentioned seeing good numbers of bright Ursids, the ZHRs were also recomputed using $r = 2.5$ as a test, but the difference in those cases where the LM was +5.5 or better, and cloud cover $< 20\%$, was negligible. Too few meteors (102 Ursids seen in $11.3^{\rm h}$) were reported for magnitude analyses unfortunately. The raw radio results were analysed as usual in previous of these results' articles.

2 Results

Almost all the visual data were from December 21–22 only. The small amount apart from this suggested very low to no Ursid activity the night before. Coverage was patchy too, but ZHRs seemed surprisingly stable for all that, averaging 17 ± 2 between $03^{\rm h}$–$14^{\rm h}$ UT. The outlying values, where at least 10 Ursids per hourly bin were available for the computation, were 12 ± 4 in the $12^{\rm h}$ UT bin, and 22 ± 6 around $05^{\rm h}$ UT. The main problem was the 'North Atlantic gap' in reports, with no usable data between roughly $05^{\rm h}30^{\rm m}$–$10^{\rm h}30^{\rm m}$ UT, because North American observers had to wait until moonset, a couple of hours or so before dawn twilight, before they could collect good enough data. The most reliably-observed interval was the hour centred at $13^{\rm h}$ UT, when three independent American watchers spotted amazingly consistent Ursid activity, right on the mean, at 17 ± 3. There was nothing to indicate any stronger peaks within the available intervals, albeit the overall ZHR was somewhat above the usual ~ 10 level. Previous Ursid outbursts have yielded ZHRs around 30–50 by comparison.

The radio data gave support for an Ursid maximum at some stage between about $09^{\rm h}$–$15^{\rm h}$ UT on December 22 (in 9 of the 11 operational systems providing useful results). The more likely peak interval within this was probably sometime between $12^{\rm h}$–$14^{\rm h}$ UT, but it was not strongly confirmed by a majority of the reports at any more specific time than this. Oddly, although the radiant was circumpolar from all the radio observing sites employed, it was almost exclusively the European systems which found something more convincing close to this midday UT timing. In North America, a possible peak nearer $00^{\rm h}$–$01^{\rm h}$ UT was suggested by two of three observers, as also by one European receiver, while several European datasets showed a good response near

the time of the radiant's local culmination, between 06^{h}–08^{h} UT. This latter might tally with the expected normal maximum.

3 Conclusion

Overall, there was support for mildly enhanced Ursid activity about as predicted by Lyytinen and Nissinen in both the visual, and more especially the radio, results. Certainly Ursid rates seemed to hold at a fairly consistent level for longer than normal in the visual reports, which may have been an indication of a general, if weakly, increased background level this year. Typically for the Ursids, too few results were received to make especially definite statements practical.

History

Meteor Beliefs Project: a second anniversary entertainment

Alastair McBeath[1] *and Andrei Dorian Gheorghe*[2]

Three unusual media reports concerning the public perception of meteoric topics, and felt appropriate for April 1st, are presented on the occasion of the Meteor Beliefs Project's second anniversary.

Received 2005 February 6

1 Introduction

Although not quite in the tone of humour set by our first Meteor Beliefs Project anniversary article in *WGN* **32:2** last year, because practical jokes and unusual or unbelievable stories are also linked with All Fools' Day, April 1, we thought the following three somewhat odd, more-or-less meteoric, items would form an appropriate piece to celebrate the Project's second anniversary with. Scientists generally often complain about the media's misperception or misunderstanding of their chosen fields, and it is certainly true that the media often acts as little more than a rumour-mill where such topics are concerned. However, it also reflects in part the public perception of those same sciences, no matter how inaccurate that may be. Since how people perceive meteors, what they think them to be and to be capable of, forms the core of the Meteor Beliefs Project, it is just as interesting to see how those beliefs are expressed today as in the distant, and not so distant, past.

The three items we have picked were collected from messages circulated on the Cambridge Conference Network (CCNet) e-mail list at various times over the last three years. The appropriate CCNet reference is given with each, and all CCNet items up to December 2003 can be found in the indexed archive at `http://abob.libs.uga.edu/bobk/cccmenu.html`. In each case, we have given a few additional or explanatory comments too, where these were felt relevant.

2 'Mystery Fireball Phenomenon A Damp Squib'

From CCNet 123/2002, circulated 2002 October 28. On October 22, the Reuters newsagency reported around half a million people had gathered along a 10 km stretch of the banks of the River Mekong in north-central Thailand the previous evening, on the Thai-Laos border near the town of Nong Khai, to view the yearly spectacle of fireballs rising from the river waters into the sky. Since the late 1940s or early 1950s, thousands of these red or pink fireballs have been seen shooting into the sky above the Mekong there, at full Moon in the eleventh lunar month (full Moon was indeed on 2002 October 21). They are called locally *bung fai phaya naga*, 'fireballs of the naga'.

Nagas are mythical giant serpents or dragons, found in various forms, including half-human kinds, across South-East Asia. They probably derived from Hindu and Buddhist originals in India, but each country seems to have subsequently developed its own types. Local Thai myths describe an ancient water-world that lies within the Mekong, where nagas live.

In 2002, the numbers of people flocking to see the spectacle was around four to five times normal, owing to the release in Thailand of a new movie on the subject, which although great for the local tourist trade, created a good many problems too. Worst of all was that only a few dozen fireballs were seen that year, leading to much disappointment and complaint among the hundreds of thousands of visitors.

Although the origin of the fireballs is said to be a mystery, and a theory concerning the release of natural gas from the river bed has been proposed, there is a competing theory that this is all a hoax, and that the fireballs are simply fireworks let off in neighbouring Laos. In this regard, we note that the capital of Laos, Viangchan (sometimes called Vientane), is on the banks of the Mekong directly opposite the province of Nong Khai, and that there was a four-hour torrential rainstorm beginning soon after sunset on 2002 October 21 ...

3 'Meteorite Shower Caused Lesotho "Poltergeist"'

In CCNet 41/2003, distributed on 2003 April 24. The BBC News Online service for April 22 drew attention to an article in the then-current BBC *Focus on Africa* magazine, regarding an outbreak of ghost activity in the village of Boqate Ha Sofonia, Lesotho. This had occurred on 2002 July 21, following a very loud sound in the sky, heard across much of the mountainous kingdom in southern Africa. Soon afterwards, villagers were alarmed at rocks falling onto roofs, damaging walls and a plastic container. One blamed a 'thokolosi', a type of poltergeist, and sprinkled holy water around her home, and on the stone that had landed in front of it, after which no further stones fell.

Several other villagers kept the stones that had struck their houses too, luckily, as it transpired they were fragments of a large meteorite shower, parts of which were recovered from nine different villages. A team from Lesotho's National University investigated, and enlisted help from villagers and school children, permitting the recovery of more than 400 pieces up to

[1]12a Prior's Walk, Morpeth, Northumberland, NE61 2RF, England, UK. Email: `meteor@popastro.com`

[2]Bd. Tineretului 53, bl. 65, ap. 40, sect. 4, Bucureşti, Romania. Email: `sarm@romwest.ro`

a kilogramme in weight. The brief notes contained in the CCNet item made no mention as to the meteorite's type, but indicated the original mass was probably of the order of a tonne, and mentioned the fall had been named Thuathe, which should hopefully enable anyone interested to still follow-up this story.

4 'Iranian January 2 Fireball Was Not A Meteorite Fall'

Contained in CCNet 21/2004, published 2004 February 12, from a press release issued by *Nojum* ('Astronomy') magazine. Following the report of a suspected meteorite fall on the town of Babol, near the southern shore of the Caspian Sea in Iran on 2004 January 2, a team organised by *Nojum* went to investigate. Although there were no professional scientists or meteorite specialists among them, they were all either amateur astronomers, science journalists or teachers.

Initial details were odd, with some sort of seismic effect noted first, then a sound was heard, followed by an unusual light seen inside a house coupled with an explosion, a loud noise, and finally the falling of a fireball which threw out sparks and was described as a 'suspended lightning' around 2 m in diameter, which suddenly vanished. The first person outdoors, who also saw the fireball, was a boy, who had his face burnt, apparently by the fireball.

The house at the centre of all this had been badly damaged by the explosion, and houses up to several hundred metres away had also taken at least some minor damage from the event. No meteorite fragments were found. Although no reason was stated in the press release, the possibility of a gas or similar explosion was excluded. Again without explanation, an unstated geophysical origin for the event was proposed, and Dr Andrei Ol'khovatov in Moscow was contacted, as he runs a webpage detailing similar unexplained fireball events that are not associated with meteorite falls (`http://olkhov.narod.ru/gr1997.htm`). Dr Ol'khovatov referred to these as 'geometeors', short for 'geophysical meteors'. The description given suggested these are some unidentified, and little-known, forms of high-speed ball lightning, statistically associated with thunderstorms. Unfortunately for this theory, the sky was clear on archived satellite images at the time of the Babol event, and no further details on what it might have been were given.

Two additional 'fireballs-that-weren't-meteors' were reported too, but these were both on stormy nights. At Marzanabad in northern Iran on 2003 May 23, a 'high speed fireball' smashed through two trees before continuing on its way, during a major thunderstorm. The electricity supply to the village was cut off for several hours afterwards. On 2004 January 21 near Meshkin Shahr in the mountains of north-west Iran, a large white fireball, 'bigger than full moon' was seen in the sky for a few minutes before disappearing. At the same time, there was a power cut across the whole area for some hours, and although no mechanism was mentioned (we presume an unstated link with the 'fireball' was intended to be assumed) a house was damaged, losing part of its roof, and having one wall plus a door damaged 'with a loud sound'. Again the night was very stormy. The press release concluded that these latter two events were probably due to 'ordinary' ball lightning.

What fascinated us particularly in this item was how unsupported and unconnected ideas were laced together to produce what might at first seem an explanation for whatever happened at Babol. While of greater interest to those investigating various electrical or electro-meteorological phenomena than meteoric/meteoritic ones, it does point up how beliefs about meteors can come about, and helps explain partly why witnesses may insist a genuine, glowing, meteoric fireball seen low in the sky 'definitely landed in the next field', despite the fact that they are still alive to make such a report.

5 Conclusion

Remember, we are always happy to see new items for potential inclusion in the Meteor Beliefs Project. We would like to continue the concept of introducing elements of humour, or quirky items like these above, in the April Project notes especially, so if you come across anything suitable, do please share it with us. Remember, the Project can only ever be as good as you help make it.

The International Meteor Organization

web site http://www.imo.net

Council

President: Jürgen Rendtel,
Eschenweg 16, D-14476 Marquardt, Germany.
tel. +49 33208 50753
e-mail: jrendtel@aip.de
Vice-President Alastair McBeath
12A Prior's Walk, Morpeth,
Northumberland NE61 2RF, UK.
tel. +44 1670 518487
e-mail: meteor@popastro.com
Secretary-General: Robert Lunsford
161 Vance Street, Chula Vista,
CA 91910-4828, USA. tel. +1 619 585 9642
e-mail: lunro.imo.usa@cox.net
Treasurer: Ina Rendtel
Mehlbeerenweg 5, D-14469 Potsdam, Germany
tel. +49 331 520 707
e-mail: IRendtel@t-online.de
Postal (giro) account number: 5472 34-107
Bank code: 100 100 10 Postbank Berlin
When paying, state bank code and postbank as well as account number!
BIC: PBNKDEFF
IBAN: DE86 1001 0010 0547 2341 07.

Other council members:
Rainer Arlt, Friedenstraße 5, D-14109 Berlin, Germany. e-mail: rarlt@aip.de
David Asher, Armagh Observatory, College Hill, Armagh BT61 9DG, Northern Ireland, UK.
e-mail: dja@star.arm.ac.uk
Malcolm Currie, 25, Collett Way, Grove, Wantage, Oxfordshire OX12 0NT, UK.
e-mail: mjc@star.rl.ac.uk
Marc Gyssens, Heerbaan 74, B-2530 Boechout, Belgium. e-mail: marc.gyssens@luc.ac.be
André Knöfel, Habichstraße 1,
D-15526 Reichenwalde, Germany.
e-mail: aknoefel@minorplanets.de
Sirko Molau, Abendstalstraße 13b,
D-84072 Seysdorf, Germany.
e-mail: sirko@molau.de
Mihaela Triglav-Čekada, Streliška 9,
SI–1000 Ljubljana, Slovenia.
e-mail: mtriglav@yahoo.com

Commission Directors

FIreball DAta Center: André Knöfel
Photographic Commission: Marc de Lignie
Steve Bikostraat 298,
NL-3573 BH Utrecht, The Netherlands
e-mail: m.c.delignie@xs4all.nl
Radio Commission: vacant
Telescopic Commission: Malcolm Currie
Video Commission: Sirko Molau
Visual Commission: Rainer Arlt

WGN

Editor: Chris Trayner
32 Moor Park Villas, Leeds LS6 4BZ, UK
fax: +44 113 3432032; mark "for C. Trayner"
tel: +44 113 2302687 e-mail: wgn@imo.net ;
include METEOR in the e-mail subject line
Editorial board: R. Arlt, M. Gyssens, A. McBeath, J. Rendtel, M. Triglav-Čekada.
Advisory board: D.J. Asher, M. Beech, P. Brown, M. Currie, M. de Lignie, W.G. Elford, R.L. Hawkes, D.W. Hughes, J. Jones, C. Keay, G.W. Kronk, R.H. McNaught, P. Pravec, G. Spalding, M. Šimek, I. Williams.

IMO Sales

Available from the Treasurer	€	$
Proceedings of the International Meteor Conference		
1990–1996	5	5
1997	Out of print	
1998–2000, 2002–2003	6	6
2001 — on CD only	5	5
2004	8	8
Back issues of WGN		
Vols. 19–22 (1991–1994) per complete volume	10	10
Vols. 23–29 (1995–2001) per complete volume	18	18
Vol. 30 (2002) per complete volume	20	20
WGN Observational Report Series		
Vols. 1–5 (1988–1992), 7–8 (1994–1995) Visual Observations, per volume	8	8
Vol. 6 (1993) Visual Observations and Electrophonic Fireball Catalogue	8	8
Vols. 9–14 (1996–2002) Visual Observations, per volume	10	10
Other publications		
Photographic Meteor Database (1986)	4	4
Photographic Astrometry + diskette	7	7

ISBN 2-87355-015-5

Proceedings of the International Meteor Conference

Varna, Bulgaria
23 - 26 September 2004

Published by the International Meteor Organization 2005

edited by
Mihaela Triglav-Čekada, Javor Kac, Alastair McBeath